Paleoecology and paleoenvironment of the Early Cretaceous theropod-dominated ichnoassemblage of the Los Corrales del Pelejón tracksite, Teruel Province, Spain

Diego Castanera[1*], Marcos Aurell[2], José Ignacio Canudo[2], Gloria Cuenca-Bescós[2], José Manuel Gasca[3], Beatriz Bádenas[2]

1: Fundación Conjunto Paleontológico de Teruel-Dinópolis/Museo Aragonés de Paleontología, Avenida de Sagunto s/n, 44002 Teruel, Spain

2: Aragosaurus—IUCA, Facultad de Ciencias, Universidad de Zaragoza, 50009 Zaragoza, Spain.

3: Departamento de Geología, Universidad de Salamanca, 37008 Salamanca, Spain

*corresponding author

Keywords: dinosaur tracks, theropod, ornithopod, splay deposits, Galve sub-basin, Teruel province

Abstract

The earliest Cretaceous (mid-late Berriasian) tracksite *Los Corrales del Pelejón* is an important dinosaur trackway site in Teruel Province in Spain. The ichnoassemblage occurs in the Galve Formation (Maestrazgo Basin) and comprises around 40 tracks assigned to theropods and ornithopods. In this paper, we undertake a paleoenvironmental analysis of the succession, which includes the overbank deposits of a fluvial environment, and discuss the implications of these findings for trackway preservation and orientation. The track-bearing unit is composed of fine- to very fine-grained, thinly bedded sandstone layers with wave ripples and traces of the *Mermia* ichnofacies, which were deposited as splay deposits within an ephemeral overbank pond. Two different theropod ichnotaxa (*Megalosauripus* cf. *transjuranicus* and Grallatoridae indet.) of three different size classes occur as small-, medium-, and large-sized tracks. The ornithopod tracks are classified as cf. *Iguanodontipus* isp. Five theropod trackways (*M.* cf. *transjuranicus*) show a bimodal orientation pattern with a similar orientation to NW-SE wave ripple crests, suggesting that these animals were walking parallel to the shoreline of the ephemeral overbank pond. Three of them walked in a similar subparallel orientation, but there is no evidence suggesting gregarious behavior as they have slightly different orientations and/or speed values. The *Los Corrales del Pelejón* site is an example of environmental influence on dinosaur behavior.

1. Introduction

Galve (Teruel Province, NE Spain) is a key locality for the analysis of Upper Jurassic-Lower Cretaceous units within the Maestrazgo Basin both in terms of its stratigraphy and its paleontological richness in vertebrates, including dinosaurs (e.g., Ruiz-Omeñaca et al., 2004; Aurell et al., 2016). Within the paleontological record of Galve, the ichnological richness stands out, with several dinosaur tracksites discovered across the different Upper Jurassic-Lower Cretaceous units. The *Los Corrales del Pelejón* tracksite studied in the present work was found in 1981 and represented the first dinosaur tracksite discovered both in Teruel Province and the Maestrazgo Basin (Casanovas et al., 1983-84; Pérez-Lorente, 2009). It also constitutes one of the first dinosaur tracksites reported in Spain, just a few years after the discoveries made in the Cameros and Asturian basins (Casanovas Cladellas and Santafé Llopis, 1971; García-Ramos, 1977; Aguirrezabala and Viera, 1980). *Los Corrales del Pelejón* is one of the main sites in the Maestrazgo UNESCO Global Geopark prepared for tourist visits (Pérez Lorente, 2009; Alcalá and Cobos, 2021). In the first investigation of the site (Casanovas et al., 1983-84), six dinosaur footprints attributed to medium to large theropod dinosaurs were identified. Cleaning and excavation of the tracksite in 1992 allowed Cuenca-Bescós et al. (1993) to provide data on 35 newly discovered tracks and seven trackways (six attributed to theropods and one to an ornithopod dinosaur).

The number of dinosaur tracks recognized in the Maestrazgo Basin has notably increased in recent years, with several localities with dinosaur tracksites described in Upper Jurassic (Kimmeridgian-Tithonian) and Lower Cretaceous (mainly Barremian) units (e.g. Pérez-Lorente, 2009; Alcalá et al., 2016; Castanera et al., 2016a, 2022; Gasca et al., 2017; Campos-Soto et al., 2019; Alcalá and Cobos, 2021; García-Cobeña et al., 2023). By contrast, the *Los Corrales del Pelejón* tracksite is the only dinosaur tracksite from the Berriasian record discovered so far in the Maestrazgo Basin (Aurell et al., 2016, 2019 and references therein). Its age is significant not only at basin scale but also globally since the Berriasian-Valanginian is a rather poorly known period in terms of dinosaur tracksites in Europe, in contrast with the large number of dinosaur tracks described in the Kimmeridgian-Tithonian (e.g., Marty, 2008; Piñuela, 2015; Piñuela et al., 2016; Razzolini et al., 2017; Rauhut et al., 2018; Castanera et al., 2018a, 2020, 2021; Belvedere et al., 2019) and Lower Cretaceous post-Valanginian units (e.g., Hernández-Medrano et al., 2008; Pérez-Lorente, 2015). The main areas with Berriasian-Valanginian dinosaur tracks are located in the Cameros Basin (Hernández-Medrano et al., 2008; Castanera et al., 2018b; Torcida Fernández-Baldor et al., 2021), the Lower Saxony Basin (e.g., Hornung et al., 2012, 2016; Richter et al., 2016), and the Wealden of the UK (e.g., Shillito and Davies, 2019).

Despite its scientific and heritage interest, the *Los Corrales del Pelejón* dinosaur tracksite has not been described in detail, especially in terms of its ichnodiversity and the paleoecological and paleoenvironmental inferences that can be drawn. In particular, Cuenca-Bescós et al. (1993) identified trackways with parallelism but a variety of directions and proposed (among other possibilities) a possible paleogeographic influence on their orientation. The hypothesis of paleogeographic barriers controlling trackway orientations has also been proposed in other cases in different areas (Lockley et al., 1986; Moratalla and Hernán, 2010; Razzolini et al., 2016; Getty et al., 2017). Nevertheless, when certain trackway parameters are also present (e.g., similar orientations, speed, and preservation), parallelism might indicate gregarious behavior (e.g., Castanera et al., 2011, 2014; García-Ortíz and Pérez-Lorente, 2014; Heredia et al., 2020).

This paper aims to provide an update on *Los Corrales del Pelejón* with an emphasis on integrating a detailed ichnological and sedimentological analysis of the site in order to: 1) analyze track preservation and ichnotaxonomy through the possible presence of one or more track-bearing layers; and 2) provide a paleoenvironmental reconstruction of the tracksite with a view to inferring whether the orientation of the trackways shows a paleoenvironmental or paleoecological (e.g., gregarious behavior) influence. The results are relevant both in adding to what is known of this significant and historic site in Spain, and enlarging the poorly known Berriasian dinosaur track record in Europe.

2. Geographical and geological setting

The *Los Corrales del Pelejón* tracksite is located near the village of Galve, a traditional dinosaur village in Teruel Province (NE Spain). The tracksite is located ca. 5 km to the southeast of the village, at the coordinates 40° 37' 30.49'' N; 0° 50' 48.10'' W.

The Upper Jurassic and Lower Cretaceous units outcropping in the Galve area belong to the Galve sub-basin, located on the western margin of the Maestrazgo Basin (Fig. 1) (Martín-Chivelet et al., 2019). The tracksite is located on the eastern flank of the Galve syncline within the lower part of the siliciclastic Galve Fm (Aurell et al., 2016). This lithostratigraphic unit has been correlated in other works (e.g., Royo-Torres et al., 2014; Campos-Soto et al., 2019) to the upper part of the Villar del Arzobispo Fm defined in the nearby South Iberian Basin (Mas et al., 1984). The Galve Fm forms part of the so-called syn-rift sequence-1 (Fig. 1C) and is irregularly recorded (from 0 to 100 m) across the eastern and western margins of the Galve sub-basin due to synsedimentary normal fault activity. In the Galve syncline, the unit consists of up to 60–80 m of red mudstones with intercalations of dm- to m-thick cross-bedded and tabular-burrowed sandstones and locally hydromorphic soils, representing fluvial channels and overbank deposits (Aurell et al., 2016, 2019).

The age of the Galve Fm in the Galve syncline is constrained to the Berriasian-early Valanginian by the presence of a sporomorph assemblage located in the lower part of the unit at the Las Zabacheras 1 fossil site (see Fig. 1A; Santos et al., 2018). The Berriasian-Barremian ostracod *Theriosynoecum fittoni* has also been found in the upper part of the unit (Aurell et al., 2019). Furthermore, in the Aliaga-Molino Alto section the recorded charophyte association suggests an age around the early to late Berriasian transition for the onset of the sedimentation of the unit in that area. According to this dataset and the sequence-stratigraphic framework (Aurell et al., 2019; Martín-Chivelet et al., 2019), the *Los Corrales del Pelejón* tracksite is probably mid-late Berriasian in age (Aurell et al., 2016, 2019).

3. Materials and methods

To analyze the sedimentological context of the tracks, a detailed stratigraphic-sedimentological analysis of the lower part of the Galve Fm was carried out in the outcropping area of the unit around the *Los Corrales del Pelejón* tracksite (Fig. 1A). This analysis encompassed: 1) a revision of the reference section of the unit established previously in this area (*Pelejón* section; Aurell et al., 2016); 2) a bed-by-bed analysis of a new stratigraphic section (*Los Corrales del Pelejón* section) in the specific area of the *Los Corrales del Pelejón* tracksite located ca. 330 m away from the reference section;

and 3) a detailed, cm-thick analysis of the track-bearing beds. Paleocurrent measurements and grain size analysis (12 samples of muddy and sandy lithologies) using a Malvern Mastersizer 3000 laser diffractometer (see results in S3) were carried out in the *Los Corrales del Pelejón* section, to complement the data obtained previously. The physical tracing of key beds and orthoimages allowed the two sections to be correlated.

The surface of the tracksite was photogrammetrically documented. A total of 585 photographs were taken with a Canon EOS 450D to cover the whole surface, and a 3D model was built using the software Agisoft Photoscan Standard Edition. Several orthophotos of the whole surface were taken using the software ZBrush and CloudCompare, allowing a new map of the tracks and trackways of the site to be drawn. This map was compared with that of Cuenca-Bescós et al. (1993). Each footprint was labeled with an acronym formed by the initial letters of the tracksite (CP), followed by the number of the trackway (e.g., CP1) and the number of the track (e.g., CP1.1 = trackway 1, track 1). Those individual tracks not arranged in trackways were numbered consecutively (e.g., CP8, CP9, etc.).

For each track, the morphological preservation (MP) was evaluated according to the scale of Marchetti et al. (2019), and the descriptions were based on those specimens with the highest MP values (avoiding extramorphological features in the descriptions). The open nomenclature follows the recommendations of Bengston (1998). Each track was analyzed individually by measuring footprint length (FL), footprint width (FW), the length and width of digits II (LII, WII), III (LIII, WIII), and IV (LIV, WIV), the “heel” (metatarsophalangeal) area (HA), and the divarication angles (II^III, III^IV) following previously used procedures (e.g., Castanera et al., 2020, 2021). The FL/FW ratio, LIII/FL, and the mesaxony (AT) were calculated accordingly. LIII/FL was calculated following Lockley et al. (2021) and Xing et al. (2021a). AT was calculated as the ratio between the anterior triangle length (ATl) and the anterior triangle width (ATw), following Lockley (2009). Different size classes were distinguished following Marty (2008) on the basis of the pes footprint length (FL) as: (1) minute = FL < 10 cm; (2) small = 10 cm < FL < 20 cm; (3) medium = 20 cm < FL < 30 cm; and (4) large = 30 cm < FL < 50 cm. Trackway data were characterized by measuring pace length (PL), stride length (SL), pace angulation (PA), trackway width (TW), and width of angulation pattern (WAP) measured from the midpoint of the footprint. Locomotion speed was estimated to compare the relative values among the trackways. The hip height (h) and the locomotion speed (v) were estimated using Alexander's (1976) formulas: hip height (h) = 4FL; speed (v) = 0.25 $g^{0.5}*SL^{1.67}*h^{-1.17}$, where g = 9.8 and is the acceleration due to gravity, and SL = stride length. We also calculated the speed according to the formula v = 0.226 $g^{0.5}*SL^{1.67}*h^{-1.17}$, as proposed by Ruiz and Torices (2013) and Navarro-Lorbés, (2021). The values of SL and h used in the formulas were mean values for each trackway. The measurements were taken with the software ImageJ from false-color depth maps in the case of the individual tracks, and in situ in the tracksite for the trackway data. The false-color depth maps were obtained from the 3D models generated from pictures taken of individual tracks with a SONY ILCE-5000, using Agisoft Photoscan Standard Edition. The scaled meshes were exported as OBJ files and then processed in CloudCompare (v.2.7.0) to obtain the false-color depth maps using the color schemes provided by Belvedere (2020). It should be emphasized that there are two different photogrammetries, one for the orthomosaic and a detailed one to characterize each individual footprint. The photogrammetric meshes of individual tracks used in this study are available for download in the supplementary information (link to be included), following the recommendation of Falkingham et al. (2018). The orientation of the trackways was plotted in a rose diagram using the software GeoRose (http://www.yongtechnology.com/download/georose).

4. Results

4.1. Facies analysis

In the study area, the Galve Fm is ~65 m thick, although its thickness varies laterally due to synsedimentary normal fault activity (Aurell et al., 2016). The stratigraphic successions of the lower part of the unit in the *Pelejón* and *Los Corrales del Pelejón* sections are shown in Figure 2A. Physical tracing and orthoimages allowed the lateral continuity of some sandstone packages to be deciphered (G1 to G7 in Fig. 2A) and a normal fault controlling variations in thickness to be identified, from ca. 30 m in *Pelejón* to ca. 18.5 m in *Corrales del Pelejón*. Packages G1 to G3 are only present in the thicker *Pelejón* section, whereas packages G4 to G7 are laterally continuous, although with lateral facies variations. The *Los Corrales del Pelejón* tracksite is located in package G6 in the *Los Corrales del Pelejón* section (Fig. 2A). The differentiated facies (Fig. 2A) are in accordance with those previously identified and interpreted as fluvial channels and overbank deposits by Aurell et al. (2016), but they are here described and interpreted in more detail (see Supplementary data S1 to S3 for detailed descriptions and interpretations) to provide a new paleoenvironmental scheme of the unit for the studied area (Fig. 2B).

The unit is dominated by red to ocherish mudstones accumulated in a sparsely vegetated floodplain, with local ponds (gray mudstones). The intercalated cross-bedded sandstones and laminated and/or bioturbated sandstones that are laterally related (e.g., G5 and G6 in Fig. 2A, see Supplementary material S1 and S2) correspond to fluvial channels and splay deposits, respectively. Paleocurrents indicate that the fluvial channels were very variable in orientation, but mainly ran southward (parallel to the orientation of the Galve sub-basin). The paleocurrents of the splay deposits are NE-directed (Fig. 2). The *Los Corrales del Pelejón* tracksite is judged to correspond to laminated and/or bioturbated splay deposits accumulated in an ephemeral pond, as 1) they are laterally equivalent to channel deposits in package G6, 2) they are overlying gray mudstones (pond deposits), and 3) they present wave ripples (Figs. 2A. B). In particular, four cm-thick, fine to very fine sandstone layers can be distinguished in the surface of the tracksite (layers 1 to 4 in Fig. 3A), including parallel-laminated layers 1 and 4 and rippled layers 2 and 3. Two main sectors (A and B) can be differentiated in the tracksite (see Figures 3 and 4). In sector B, it is mainly layer 1 that crops out due to current erosion of the overlying layers. In sector A, the four layers can be distinguished, except in some areas where ripples disappear laterally (Fig. 3A, D). These ripples are asymmetric and symmetric wave ripples (with bifurcation, zig-zag, and hourglass crest morphology; e.g., Perron et al., 2018) and are present in the very fine sandstone layers 2 and 3 (Fig. 3), thus reflecting subaqueous deposition and a NW-SE paleowind direction (Fig. 2). Several invertebrate traces can be identified in the different layers of the tracksite. Simple horizontal (e.g., *Helminthopsis*, *Gordia*) and vertical burrows are present in layer 1. The rippled layer 3 is characterized by arthropod trackways (e.g., *Diplopodichnus*), simple horizontal burrows and trails (e.g., *Helminthopsis*, *Helminthoidichnites*), and simple vertical burrows. The topmost very fine sandstone layer 4 (presumably the dinosaur tracking surface) has parallel lamination and an exclusive presence of grazing trails (indeterminate and simple horizontal trails of

Helminthopsis). Floodplain red mudstones cover the track-bearing beds (Fig. 3A). This invertebrate ichnoassemblage, with its rather low ichnodiversity, represents an example of the *Mermia* ichnofacies, characterized by a predominance of horizontal grazing traces produced in low-energy environments such as floodplain ponds and under subaqueous conditions (Buatois and Mangano, 2011; Melchor et al., 2012). Bioturbation traces are recorded close to some tracks, but there is no clear evidence to decipher their cross-cutting relationships, especially in layer 4, so it is difficult to infer whether the dinosaur tracks and the invertebrate traces were coeval or not.

4.2. Track preservation

Around 40 dinosaur tracks are identified in the *Los Corrales del Pelejón* tracksite, including five clear theropod trackways (CP1, CP2, CP3, CP5 and CP6) (Fig. 4). As well as this, three pairs of two tracks might be part of two different trackways (CP4 and CP7). In addition, some isolated tridactyl tracks (CP8-C11) and four large, rounded depressions (CP12-CP15) of indeterminate origin (possibly undertracks) are identified. Most of these tracks were previously reported by Cuenca-Bescós et al. (1993), except for the first tracks in trackways CP1-CP3 and track CP6.5, which were unearthed in cleaning operations and excavations carried out in subsequent years. Tracks CP10 and CP11 can only be identified under certain light conditions. All the tracks are preserved as concave epireliefs. Trackways CP1 and CP2, and track CP11, are located in Sector A of the tracksite (left side of the map in Fig. 4), and the tracks are mainly preserved on top of layers 4 and 3 (e.g., CP2, Fig. 3B). In the upper area of sector A, where rippled layers 2 and 3 change laterally to the topmost part of layer 1 (Fig. 3), the tracks are preserved on top of this layer (e.g., CP1.1, Fig. 3B). By contrast, in sector B (right side of the map in Fig. 4), trackways CP3 to CP7 and isolated tracks CP8 to CP10 are preserved on top of layer 1 (Fig. 3), and the overlying layers are absent. The observed track preservation thus indicates that all the dinosaurs possibly impressed their footprints on layer 4 (this layer would be the original tracking surface), so trackways CP1 and CP2 are preserved as true tracks, and those preserved in the underlying layers (e.g., trackways CP3 to CP7 and isolated tracks CP8 to CP10) are shallow undertracks. This interpretation is also in accordance with the MP values, which are higher in trackways CP1 and CP2 (see Table 1, Fig. 4C, Fig. 5).

4.2 Dinosaur morphotypes

4.1.1 Theropod tracks

Based on footprint size and morphology, two different theropod morphotypes of three different size classes can be distinguished (Table 1): one small-sized (CP4, FL = 15.5 cm, Fig. 5K), one medium-sized (CP1, CP5, CP9, CP10; FL = 26-28 cm, Fig. 5A-B, G-H, J), and one large-sized (CP3 and CP6, FL = 35, 39 cm, Fig. 5C-F, I). The tracks are tridactyl and notably gracile, showing differences between the different size classes, especially in the FL/FW ratio and mesaxony. Generally, the smaller specimens have higher values for FL/FW and mesaxony (CP4.1-CP4.2 = 1.53-1.63/0.66-0.74) than the medium (CP1.1-CP1.4 = 1.48-1.64/0.56-0.6; CP5.1 = 1.54/0.6) and larger specimens (CP2.4-CP2.5 = 1.44-1.43/0.48-0.55; CP3.3 = 1.61/0.57; CP6.2 = 1.57/0.55). The tracks with higher morphological preservation values are characterized by a large, rounded, metatarsophalangeal pad impression, as shown in individuals of both the medium and large-sized classes (e.g., CP1.1, CP1.3, CP2.4, CP3.3, CP5.1, CP6.2). The digits are slender in all the trackways, except in CP6, where they are somewhat robust (Fig. 5I). Digit III is clearly the longest, digit IV being generally slightly longer than digit II. The digit divarication is low in the three different size classes (generally lower than 50º, see Table 1). The distal ends of the digits are acuminate, showing clear claw impressions in the best-preserved tracks (e.g., CP1.4, Fig. 5B).

4.1.2 Ornithopod tracks

CP7 is the only trackway possibly attributable to ornithopods. It is composed of two pairs of two footprints, which might represent part of the same trackway showing a slight change in direction. CP7.4 has the highest morphological quality. It is a large-sized tridactyl track (FL = 35.5 cm), slightly longer than wide (FL/FW ratio = 1.09), with medium mesaxony (AT = 0.44). The footprints are symmetrical, with a rounded to quadrangular metatarsophalangeal pad impression. The digits are robust (9 cm in width), digit III being slightly longer than digits II and IV, which are subequal in length. The hypices are symmetrical, and the digits possibly show one phalangeal pad per digit.

The distal end of the digits is rounded, without evidence of clear claw marks (indicative of blunt claws). The interdigital angle is medium (63º), and III^IV slightly higher than II^III.

4. 3 Orientation and locomotion speed values of the dinosaur trackways

The dinosaur trackways of the *Los Corrales del Pelejón* tracksite are not very long, with no more than seven footprints. They have different orientations (see Fig. 4, Table S1), showing a generally multidirectional pattern. Of the theropod trackways, CP1, CP2 and CP3 are heading to the SW, the former two being parallel and CP3 subparallel with a higher SW orientation. The three trackways have speed values close to 2 m/s (see Table S1), CP2 and CP3 having rather similar speed values. CP1 is the fastest trackway (2.15-2.37 m/s). CP6 is parallel to CP3 but is heading in the opposite direction (NE), with a slightly lower speed value (1.59-1.76 vs 1.98-2.19 m/s respectively). CP5 has a NE orientation, with the lowest speed value (1.5-1.66 m/s). CP4 is heading SE. By contrast, the ornithopod tracks in CP7 are heading NW, with a change in the direction of travel to the W from the first pair to the second pair. No speed values are calculated in the latter since there are not three consecutive tracks preserved.

In summary, although the rose diagram shows a generally multidirectional pattern of trackway directions (Fig. 4), it indicates a rather bimodal (NE-SW) pattern in the medium to large theropod trackways (CP1-CP3, CP5-CP6). It is interesting to observe that the theropod trackways are very narrow, with high pace angulations (greater than 165º, see Table S1). Also noteworthy is the difference in speed values among trackways produced by similar-sized theropods: for example, CP1 moved considerably faster (longer PL and SL and higher PA) than CP5; CP2 and CP3 moved at rather similar speeds and slightly faster than CP6. Despite these differences in speed values and the fact that according to their footprint length they can be included in the range of the "good runner" dinosaurs (see Navarro-Lorbés et al., 2021), all the theropod trackways show a rather low absolute value. Thus, they were moving with a walking gait with a low speed, as also evidenced by the low values (1.42-1.97) of their relative stride length (values lower than 2, Thulborn, 1990).

5. Discussion

5.1 Ichnotaxonomic affinities and candidate trackmakers

Some tracks from *Los Corrales del Pelejón* (CP3 and CP6, and possibly CP1.4) were previously compared by Casanovas et al. (1983-84) to various ichnotaxa such as *Eubrontes giganteus* Hitchcock, 1845 (Fig. 6A), *Eutynichnium lusitanicum* Nopcsa, 1923 (Fig. 6B), *Megalosauropus broomensis* Colbert and Merrilees, 1967 (Fig. 6C), and *Bueckeburgichnus maximus* Kuhn, 1958 (Fig. 6D). The authors noted the similarities, especially with respect to *Eubrontes*, but emphasized that this ichnotaxon is mainly found in the Upper Triassic and Lower Jurassic and so did not classify the tracks. Pérez-Lorente (2009) suggested that track CP1.4 could be classified as *Eubrontes*. Generally, *Eubrontes* tracks are indeed typical of the Late Triassic-Early Jurassic (Olsen et al., 1998; Lucas et al., 2006), but they have also been described in the Cretaceous of Asia (e.g., Xing et al., 2016, 2021). Although some of the tracks in CP3 and CP6 might resemble *Eubrontes*-like tracks (see fig. 6 in Xing et al., 2021), the heel pad impression of Cretaceous *Eubrontes* (e.g., *E. nobitai*, Fig. 6E) is bilobed with a third phalangeal pad in digit II close to the heel pad impression. In the studied theropod tracks (CP1-CP6) this pad is not present, and the heel pad impression is rounded and centered in relation to the track axis. Moreover, CP1.4 is more gracile than many of the tracks classified as *Eubrontes*.

The other three ichnotaxa mentioned by Casanovas et al. (1983-84) are now either considered *nomem dubium* or related to *Megalosauripus* Lockley, Meyer, & Santos, 1996 (Lockley et al., 1996, 2000; Belvedere et al., 2019). Certainly, both the medium and large-sized theropod tracks from *Los Corrales del Pelejón* show similarities with the tracks assigned to *Megalosauripus* (Fig. 6F-6G), which is typical of Middle Jurassic-Lower Cretaceous successions, including several sites in the Iberian Peninsula and the Maestrazgo Basin (Lockley et al., 1996, 2000; Fanti et al., 2013; Razzolini et al., 2016, 2017; Belvedere et al., 2019; Castanera et al., 2021). *Megalosauripus* tracks are characterized as being large and gracile in contrast to coeval robust and giant tracks such as *Jurabrontes curtedulensis* Marty, Belvedere, Razzolini, Lockley, Paratte, Cattin, Meyer, 2018 (Fig. 6H) or *Iberosauripus grandis* Cobos, Lockley, Gascó, Royo–Torres, Alcalá, 2014 (Fig. 6I), the latter of which is also identified in Tithonian-Berriasian units of the Iberian Range (Cobos et al., 2014; Castanera et al., 2015; Marty et al., 2018;

Belvedere et al., 2019). Two ichnospecies of *Megalosauripus* are currently considered valid (Razzolini et al., 2017; Belvedere et al., 2019; Meyer et al., 2021): *M. uzbekistanicus* Lockley, Meyer, & Santos, 1996 (Fig. 6F) and *M. transjuranicus* Razzolini, Belvedere, Marty, Paratte, Lovis, Cattin, & Meyer, 2017 (Fig. 6G). The *Los Corrales del Pelejón* tracks show greater similarities with *M. transjuranicus*, especially in their gracility and the rounded heel mark morphology. A diagnostic feature of *M. uzbekistanicus* is its elongated heel impression (Lockley et al., 2000), whereas in *M. transjuranicus* the heel impression is circular and rounded, and generally has twice the width of the rest of the dIV impression. In the tracks from *Los Corrales del Pelejón* with high MP values that do have a characteristic circular and rounded heel pad impression (e.g., CP1.1; CP1.4, Fig. 5), this is not as wide as in *M. transjuranicus* (the width is around 1.5 times the width of dIV). It should be noted that these tracks are slightly smaller than *M. transjuranicus.* This would be a difference with respect to both ichnospecies of *Megalosauripus* since generally *Megalosauripus* tracks are larger than 35-40 cm (Fanti et al., 2013; Razzolini et al., 2017).

Distinguishing between *Eubrontes* and *Megalosauripus* can be difficult when the tracks do not have high MP values. Recently, Lockley et al. (2021) suggested that the two ichnotaxa might differ in the length of digit III with respect to the length of the footprint, *Eubrontes* having a longer digit. Xing et al. (2021a) provide copious data on this parameter in different *Eubrontes*-like tracks, showing a variation from 0.57 to 0.71. The authors propose this ratio to quantify digitigrady and indicate that it is also quantitatively related to the presence or absence of a digit II metatarsal phalangeal pad. In the case of *Los Corrales del Pelejón* (see Table 1, S4), the values of this ratio vary from 0.67 (CP3.6) to 0.81 (CP2.6). In the best-preserved tracks, the ratios are between 0.70 (CP3.3) and 0.75 (CP5.3). As already mentioned, the tracks do not show any sign of the impression of the digit II metatarsal phalangeal pad, so attribution to a *Eubrontes*-related ichnotaxon is not justified. This is also reinforced by the length/width ratio and the mesaxony, *Eubrontes*-like tracks having generally lower values in both parameters (see S4).

A large, rounded heel pad impression is also a diagnostic feature of *Asianopodus*. *Asianopodus pulvinicalx* Matsukawa, Shibata, Kukihara, Koarai, & Lockley 2005, the type ichnospecies, was described from the Valanginian-Barremian of Japan (Fig. 6J).

This ichnotaxon is diagnosed by a "small to medium sized tridactyl, mesaxonic and subsymmetrical track with distinct bulbous heel impression. Track is longer than wide. The digital divarication angles are rather narrow" (Matsukawa et al., 2005). Subsequently, Li et al. (2011) described a second ichnospecies, *A. robustus* Li 2011 (Fig. 6K), from the Lower Cretaceous of Inner Mongolia. The main differences of this ichnospecies are its size and a separated heel pad impression. A third ichnospecies, *A. niui* Li, Jiang, & Wang, 2020 (Fig. 6L), was defined by Li et al. (2020) but subsequently designated a *nomen dubium* (Xing et al., 2021b, 2021c). Xing et al. (2021c) described another ichnospecies, *A. wangi* Xing, Lockley, Mao, Klein, Gu, Bai, Qiu, Liu, Romilio, Scott Parsons IV & Wan 2021, from the Berriasian of China (Fig. 6K), characterized by higher mesaxony and a longer digit III than the other ichnospecies. *Asianopodus*-like tracks have also been described in the Lower Cretaceous of Mongolia and China (Xing et al., 2014) and Argentina (Heredia et al., 2020). The overall dimensions (FL/FW ratio and mesaxony) of the *Asianopodus* ichnospecies are slightly different (see S4) from those of the *Los Corrales del Pelejón* tracks (1.43-1.6 and 0.43-0.67, in the best-preserved tracks, see Table 1) and vary between the ichnospecies (1.44/0.45 in *A. pulvinicalx*; 1.23/0.40 in *A. robustus*; 1.7/0.64 in *A. wangi*). In the *Los Corrales del Pelejón* tracks, these values vary between those of *A. pulvinicalx* (e.g., CP2) and *A. wangi* (e.g., CP1.4) (see Table 1, Table S1). Razzolini et al. (2017) noted that *M. transjuranicus* and *Asianopodus* have some features in common regarding the metatarsophalangeal pad area and argued that in the latter this is located in a more central position and separated from the digit impressions (a feature not seen in *A. wangi*), the track being more symmetrical. Xing et al. (2021c) also noted the similarities between the two ichnotaxa, emphasizing that the main differences are in the heel pad, which is located "rather laterally to the digit III axis" in *Megalosauripus* and "in continuation with digit III" in *Asianopodus*. The previous considerations suggest that the medium to large *Los Corrales del Pelejón* tracks are more similar to *M. transjuranicus* and *Asianopodus wangi* than to any other ichnotaxa, although they do not strictly have all the diagnostic features of either of them. It is interesting to note that the best-preserved footprints from *Los Corrales del Pelejón* only show slight variations in the parameters despite the differences in the MP values associated with the track-bearing layers where they are preserved (tracks and shallow undertracks, with just a cm of difference between the layers in which they are preserved) (see the previous section and Fig. 3). Nonetheless, they show considerable variations in MP even within the same trackway, and only CP1.4 has an MP value higher than 2. In the light of these data, the tracks are tentatively classified as *M.* cf. *transjuranicus*. This attribution is also consistent with the length/width ratio and mesaxony as compared with the main theropod ichnotaxa in a bivariate plot (see Supplementary data S4), although the values from both *M. transjuranicus* and *Asianopodus* overlap partially. This discussion opens a new window onto the question of how properly to distinguish between *M. transjuranicus* (an ichnotaxon typical of the Kimmeridgian-Berriasian interval of Europe) and *Asianopodus* (an ichnotaxon typical of the Lower Cretaceous of Asia).

As regards the small-sized theropod (CP4) morphotype, just a few small-sized theropod ichnotaxa have been described in the Kimmeridgian-Berriasian interval of Europe. The main ichnotaxa identified in the Kimmeridgian-Tithonian include *Grallator*, *Carmelopodus*, *Wildeichnus*, cf. *Jialingpus*, and *Therangospodus*-like tracks (see Castanera et al., 2016b, 2018a and references therein). In Berriasian areas, by contrast, identified small-sized tridactyl theropod ichnotaxa are almost absent (e.g. Hernández-Medrano et al., 2008; Hornung et al., 2012), with the exception of *Kalohipus bretunensis* Fuentes Vidarte and Meijide Calvo 1998 (Fig. 6R). This latter ichnotaxon and the small-sized theropod (CP4) morphotype resemble tracks included in Grallatoridae (Lull, 1904; see Melchor et al., 2019). According to the latter authors, these footprints are characterized by moderate to marked elongation (FL/FW > 1.50) and mesaxony. The morphological quality of CP4 is rather low, but the tracks meet these parameters. Grallatorid tracks are common in the Kimmeridgian-Berriasian successions of the Iberian Peninsula (Castanera et al., 2015, 2016b, 2021), including the aforementioned *Kalohipus bretunensis* (Fig. 6R) and *Grallator* isp. (Fig. 6S). The main differences between them lie in mesaxony and the FL/FW ratio. The values of CP4 are more similar to those of *Kalohipus*, but taking into account the low MP values of the CP4 tracks they are classified as Grallatoridae indet.

The tracks of the ornithopod trackway (CP7) have a very low MP value except for CP7.4. This track has many of the diagnostic features of the ichnofamily Iguanodontipodidae (sensu Díaz-Martínez et al., 2015), such as one pad impression in each digit and the heel, the pads being longer than wide, and also well-developed notches in the proximal part of digit II and digit IV. On the other hand, the track is slightly longer than wide (not as wide as or wider than long). The track also has diagnostic features of the ichnogenus *Iguanodontipus*, such as a small, rounded, and centered heel impression that is narrow. Although the preservation of the heel mark is rather poor, it is possibly similar in width to the proximal part of digit III. Castanera et al. (2022) suggested that this track "can be considered as *Iguanodontipus*-like". *Iguanodontipus*-like tracks (Fig. 6T-6V) have been described in a variety of European Berriasian localities, including England (Sarjeant et al., 1998 and references therein), Germany (Dietrich, 1927; Hornung et al., 2012, 2016), and Spain (Castanera et al., 2013). Díaz-Martínez et al. (2015) compiled information on this ichnotaxon and concluded that *Iguanodontipus burreyi* Sarjeant, Delair, & Lockley 1998 (Fig. 6T-V) is the only valid ichnospecies within *Iguanodontipus*. Subsequently, Piñuela et al. (2016) described new tracks (Fig. 6W) from the Upper Jurassic of Asturias (Spain) and questioned the validity of *Iguanodontipus* due to the poor preservation of the holotype, even suggesting that the trackmaker might not be an ornithopod. New tracks assigned to Iguanodontipodidae have also been described in the Upper Jurassic of Portugal (Fig. 6X, Castanera et al., 2020). Given the current state of knowledge, therefore, a review of the type and the referred material of *Iguanodontipus burreyi* is needed in order properly to classify the CP7 tracks, and to understand 1) whether *Iguanodontipus* is a monospecific ichnogenus, and 2) whether the stratigraphic range of *I. burreyi* would be restricted to the Berriasian of Europe. In the light of this discussion and the fact that track CP7.4 shows slight differences with respect to the diagnostic features of the emended diagnosis proposed by Díaz-Martínez et al. (2015), we classify the CP7 tracks as cf. *Iguanodontipus* isp. Even though the tracks from *Los Corrales del Pelejón* could not be assigned with confidence to a specific ichnospecies/ichnogenus and most of them are classified in open nomenclature, the ichnoassemblage is of particular interest since it provides new data that shed light on whether or not there might be an ichnofaunal change across the Tithonian-Berriasian boundary. In the current state of knowledge, *Asianopodus* and *Iguanodontipus* are restricted to the Lower Cretaceous of Asia and Europe respectively, so further work is needed to ascertain whether these ichnotaxa are already present in the Late Jurassic (Kimmeridgian/Tithonian) or whether there might be a change in both theropod (*Megalosauripus transjuranicus*/*Asianopodus*) and ornithopod tracks (unnamed Iguanodontipodidae/*Iguanodontipus*) through the Jurassic/Cretaceous (Tithonian-Berriasian) transition.

The identity of the trackmakers of the trackways is especially difficult to ascertain due to the poor osteological record of theropods and ornithopods in the Tithonian-

Valanginian interval in the Maestrazgo and South Iberian basins. The sauropod *Aragosaurus ischiaticus* Sanz, Buscalioni, Casanovas, & Santafé, 1987 is the only dinosaur formally named in the Berriasian of the Maestrazgo Basin (Sanz et al., 1987; Canudo et al., 2012; Royo-Torres et al., 2014). Other dinosaur remains have been assigned to dromaeosaurs and stegosaurs (Ruiz-Omeñaca et al., 2004; Pereda Suberbiola et al., 2005). Theropod remains assigned to large tetanurans (possible megalosaurids), middle-sized allosaurids, and small dromaeosaurs have been described on the basis of their teeth in slightly older (Tithonian) deposits in both basins (Canudo, 2006; Gascó et al., 2012; Cobos et al., 2014). Berriasian ornithopod remains are absent in the area although Kimmeridgian-Tithonian remains have been recovered in the South Iberian Basin (Sánchez Fenollosa et al., 2022, 2023 and references therein).

The Berriasian/Valanginian theropod record in Europe is also quite sparse. Remains of the dromaeosaur *Nuthetes destructor* have been described in the Berriasian of the UK (Milner, 2002) and France (Pouech et al., 2014). Turmine-Juhel et al. (2019) reported teeth of theropod dinosaurs assigned to *Baryonyx* and to an allosauroid from the Valanginian Wadhurst Clay Formation. The largest European sample of theropod remains comes from the Berriasian of France, concretely from Angeac-Charente. Four different non-avian theropod taxa have been described based on teeth and postcranial material: cf. *Nuthetes* sp., Tyrannosauroidea indet., Megalosauridae? indet., and Ornithomimosauria indet. (Allain et al., 2022). Traditionally, Late Jurassic *Megalosauripus transjuranicus*-like tracks have been associated with allosauroids or ceratosaurs as their most plausible trackmakers (Razzolini et al., 2017; Rauhut et al., 2018; Castanera et al., 2021). With the data currently available, it is not possible to associate the *Los Corrales del Pelejón* tracks with any of the abovementioned groups, since none of the criteria proposed by Carrano and Wilson (2001) for correlations between tracks and trackmakers (synapomorphy-based, phenetic or coincidence correlations) can be confidently applied to the studied tracks.

As regards the candidate trackmaker for the ornithopod trackway CP7, Angeac-Charente is also the site with the highest diversity of ornithopod remains from the Berriasian of Europe. Remains from three different ornithopod taxa have been described in this site: teeth belonging to the heterodontosaurid *Echinodon* sp. and Hypsilophodontidae indet. and teeth and postcranial material assigned to ankylopollexians (Allain et al., 2022). The former two taxa are too small to have produced the CP7 tracks, whereas the ankylopollexians would fit better. However, the footprint length (FL> 35 cm) is slightly higher than the estimates calculated for the Late Jurassic taxa *Camptosaurus dispar* (FL = 26 cm; Gierlinski et al., 2009) and *Oblitosaurus bunnueli* (FL = 29-31 cm; Sánchez Fenollosa et al., 2023). *Iguanodontipus* tracks have usually been associated with Ankylopollexia or basal Styracosterna (Díaz-Martínez et al., 2015), so the presence of ankylopollexians in the slightly older deposits of the nearby South Iberian Basin (Sánchez Fenollosa et al., 2022, 2023) and in the Berriasian of Europe (Agneac; Allain et al., 2022) suggests by the coincidence correlation (Carrano and Wilson, 2001) that an ankylopollexian is the most plausible trackmaker for the CP7 tracks.

5.2 Paleoenvironmental and paleoecological influence on the dinosaur trackway orientations

As previously mentioned, (see section 4.1), all the dinosaurs have been interpreted as impressing their footprints on layer 4 (the interpreted tracking surface), suggesting that all the trackways were coeval. This interpretation is significant for understanding whether the trackway orientation might show any paleoenvironmental or paleoecological influence. Parallelism in dinosaur trackways has usually been used to infer gregarious behavior (e.g.: Ostrom, 1972; Castanera et al., 2011, 2014; García-Ortíz and Pérez-Lorente, 2014). In addition, some reports (Moratalla and Hernán, 2010; Razzolini et al., 2016; Getty et al., 2017) have also shown the importance of paleogeographical barriers such as ancient shorelines (either coastal or lacustrine) for the orientation of the trackways. The latter authors have shown the importance of not assuming either gregariousness or a paleogeographic barrier solely from the parallelism of the trackways. The dinosaur trackway orientations among the medium and large-sized theropod trackmakers of the *Los Corrales del Pelejón* tracksite show both a clear bimodal pattern (NE-SW) and a multidirectional but perpendicular pattern (NW-SE), where the ornithopod trackway CP7 and the small-sized theropod trackway CP4 are included (Fig. 4). The orientation of the individual tracks (CP8, CP10 and CP11) also shows rather similar directions (see Fig. 4B). Generally, a bimodal orientation pattern is associated with paleogeographic constraints/natural barriers such as shorelines, river-banks or even basin configuration (Lockley et al., 1986; Thulborn, 1990; Lockley, 1991; Moratalla and Hernán, 2010; Razzolini et al., 2016), especially when the trackways have similar directions but opposite orientations, as in the case of trackways CP1-CP2 (and tracks CP8 and CP11) vs CP5 (and track CP10) and CP3 vs CP6. Cuenca-Bescós et al. (1993) highlighted that the latter two trackways were subparallel but were moving in opposite directions, so a geographic barrier would be a possible explanation for their orientation. Ostrom (1972) even suggested “that the presence of parallel trackways in opposite directions is a starting point for suspecting the existence of some kind of physical barrier that affected the passage of individuals.” The tracks formed on layer 4 can be compared with the orientation of the ripple crests of layers 2 and 3, as the entire track-bearing package of layers 1 to 4 formed in an ephemeral pond (see section 4.1). In particular, the orientation of trackways CP1, CP2, C5, (and roughly CP3 and CP6 and the individual tracks CP8, CP10 and CP11) is similar to that of the crest of the ripple marks (NE-SW) in layers 2 and 3 (Figs. 2B, 3B). Given that the wave ripples probably formed parallel to the shoreline of the ephemeral pond, the medium and large theropods may have walked across the site parallel to this shoreline whereas the ornithopod and the small theropod walked perpendicular to it. Despite the shortness of the trackways, the six theropod trackways show a directional pattern (linear trackways), as a consequence of the dinosaurs crossing the site with no evidence of milling behavior (Cohen et al., 1993). Taking into account these data and the fact that the trackways differ in their speed values (see Table S1), it is thus plausible that the orientations of the trackways do show a paleoenvironmental influence. As regards any possible paleoecological influence, it should be highlighted that CP1 and CP2 show a parallel configuration and a close inter-trackway space (just a meter); CP2 and CP3 are subparallel and show a rather similar speed value (see Table S1). However, the slight differences in speed values, preservation, size and the inferred paleoenvironmental influence preclude the suggestion that these theropods were walking together, so there is no clear evidence of an ethological/paleoecological influence.

6. Conclusions

This analysis of the *Los Corrales del Pelejón* dinosaur tracksite in Galve has provided significant new data on the preservation and ichnotaxonomy of the tracks and the paleoenvironmental influence on the orientation of the dinosaur trackways. The tracksite is located in a sandstone package composed of four cm-thick sandstone layers, with wave ripples and simple grazing trails and burrows of the *Mermia* ichnofacies, representing splay deposits accumulated in an ephemeral pond. All the dinosaurs impressed their footprints in the uppermost layer, but the trackways are preserved in different layers, either as true tracks (layer 4) or shallow undertracks (layers 1-3). Despite the differences in morphological preservation, the tracks do not show great variation in their morphometric data, probably due to the reduced thickness of the layers. The tracks are assigned to *M*. cf. *transjuranicus* and Grallatoridae indet. (produced by indeterminate theropods) and cf. *Iguanodontipus* isp. (possibly produced by an ankylopollexian ornithopod). Analysis of the trackway orientations and paleocurrents indicates that the dinosaurs crossed the site individually and at slightly different speeds. Concretely, the medium to large theropods (CP1-CP3, CP5-CP6) were possibly walking parallel to the shoreline of the ephemeral pond, whereas the small theropod (CP4) and the ornithopod (CP7) were walking perpendicular to it. This paleogeographic constraint was thus a considerable influence on the dinosaur trackway orientations.

Acknowledgments

DC has been supported by the Beatriu de Pinós postdoctoral program (BP2017- 0195) of the Government of Catalonia's Secretariat for Universities and Research of the Ministry of Economy and Knowledge. This study was subsidized in part by Project PID2021-122612OB- I00 of the Spanish Ministerio de Ciencia e Innovación, Unidad de Paleontología de Teruel (Ministerio de Ciencia e Innovación) as well as by the Aragon Regional Government (Grupos de referencia: E04_20R FOCONTUR y E18_23R Aragosaurus: Recursos Geológicos y Paleoambientales). This research has been carried out under permissions 202/2018 and 041/19-20-2021 issued by the Dirección General de Patrimonio Cultural of the Aragon Government. The authors also acknowledge the members of the Fundación Conjunto Paleontológico Teruel-Dinopolis, Paleoymás SL and Juan Carlos García Pimienta for providing information, historic pictures of the tracksite, and/or field assistance. Ulyses Palomino built the 3D model of the tracksite, and his help is also appreciated. The help of Gabriela Mangano and Luis Buatois in the identification of invertebrate traces is gratefully acknowledged. The comments of three anonymous reviewers have improved the manuscript and are greatly appreciated.

References:

Aguirrezabala, L.M., Viera, L.I. (1980). Icnitas de dinosaurios en Bretún (Soria). Munibe, 3-4, 257-279.

Allain, R., Vullo, R., Rozada, L., Anquetin, J., Bourgeais, R., Goedert, J., ... & Tournepiche, J. F. (2022). Vertebrate paleobiodiversity of the Early Cretaceous (Berriasian) Angeac-Charente Lagerstätte (southwestern France): implications for continental faunal turnover at the J/K boundary. Geodiversitas, 44(25), 683-752.

Alcalá, L., Lockley, M. G., Cobos, A., Mampel, L., & Royo-Torres, R. (2016). Evaluating the dinosaur track record: an integrative approach to understanding the regional and global distribution, scientific importance, preservation, and management of tracksites. Dinosaur Tracks. Indiana University Press, Bloomington, Indiana, 101-117.

Alcalá, L., & Cobos, A. (2021). Dinosaur Tracksites from the Maestrazgo UNESCO Global Geopark (Teruel, Spain). Geoconservation Research, 4(2), 413-426.

Alexander, R. M. (1976). Estimates of speeds of dinosaurs. Nature, 261, 129-130.

Aurell, M., Bádenas, B., Gasca, J. M., Canudo, J. I., Liesa, C. L., Soria, A. R., ... & Najes, L. (2016). Stratigraphy and evolution of the Galve sub-basin (Spain) in the middle Tithonian–early Barremian: implications for the setting and age of some dinosaur fossil sites. Cretaceous Research, 65, 138-162.

Aurell, M., Bádenas, B., Canudo, J. I., Castanera, D., García-Penas, A., Gasca, J. M., ... & Val, J. (2019). Kimmeridgian–Berriasian stratigraphy and sedimentary evolution of the central Iberian Rift System (NE Spain). Cretaceous Research, 103, 104153.

Belvedere, M., Castanera, D., Meyer, C. A., Marty, D., Mateus, O., Silva, B. C., ... & Cobos, A. (2019). Late Jurassic globetrotters compared: A closer look at large and giant theropod tracks of North Africa and Europe. Journal of African Earth Sciences, 158, 103547.

Belvedere, Matteo (2020). CloudCompare Depth Map color schemes. figshare. Dataset. https://doi.org/10.6084/m9.figshare.11742660.v3

Bengtson, P. (1988). Open nomenclature. Palaeontology, 31(1), 223-227.

Buatois, L. A., & Mángano, M. G. (2011). *Ichnology: Organism-substrate interactions in space and time*. Cambridge University Press.

Carrano, M. T., & Wilson, J. A. (2001). Taxon distributions and the tetrapod track record. Paleobiology, 27(3), 564-582.

Casanovas-Cladellas, M.L., Santafé-Llopis, J.V. (1971). Icnitas de reptiles mesozoicos en la provincia de Logroño. Acta Geológica Hispánica, 139-142.

Casanovas-Cladellas, M.L., Santafé-Llopis, J.V., Sanz, J.L. 1983-84. Las Icnitas de "Los Corrales del Pelejón" en el Cretácico Inferior de Galve (Teruel, España). Paleontologia i Evolució, 18, 155-162.

Castanera, D., Barco, J. L., Díaz-Martínez, I., Gascón, J. H., Pérez-Lorente, F., & Canudo, J. I. (2011). New evidence of a herd of titanosauriform sauropods from the lower Berriasian of the Iberian range (Spain). Palaeogeography, Palaeoclimatology, Palaeoecology, 310(3-4), 227-237.

Castanera, D., Pascual, C., Razzolini, N. L., Vila, B., Barco, J. L., & Canudo, J. I. (2013). Discriminating between medium-sized tridactyl trackmakers: tracking ornithopod tracks in the base of the Cretaceous (Berriasian, Spain). PloS one, 8(11), e81830.

Castanera, D., Vila, B., Razzolini, N. L., Santos, V. D., Pascual, C., & Canudo, J. I. (2014). Sauropod trackways of the Iberian Peninsula: palaeoetological and palaeoenvironmental implications. Journal of Iberian Geology, 40(1), 49-59.

Castanera, D., Colmenar, J., Sauque, V., & Canudo, J. I. (2015). Geometric morphometric analysis applied to theropod tracks from the Lower Cretaceous (Berriasian) of Spain. Palaeontology, 58(1), 183-200.

Castanera, D., Díaz-Martínez, I., Moreno-Azanza, M., Canudo, J. I., & Gasca, J. M. (2016a). An overview of the Lower Cretaceous dinosaur tracksites from the Mirambel Formation in the Iberian Range (NE Spain). New Mexico Museum of Natural History and Science Bulletin. Cretaceous period: biotic diversity and biogeography, 71, 65-74.

Castanera, D., Piñuela, L., & García-Ramos, J. C. (2016b). *Grallator* theropod tracks from the Late Jurassic of Asturias (Spain): ichnotaxonomic implications. Spanish Journal of Palaeontology, 31(2), 283-296.

Castanera, D., Belvedere, M., Marty, D., Paratte, G., Lapaire-Cattin, M., Lovis, C., & Meyer, C. A. (2018a). A walk in the maze: variation in Late Jurassic tridactyl dinosaur tracks from the Swiss Jura Mountains (NW Switzerland). PeerJ, 6, e4579.

Castanera, D., Pascual, C., Canudo, J. I., & Barco, J. L. (2018b). Bringing together research, geoconservation and reaching a broad public in the form of a geotourism project: the Ichnite Route of Soria (Spain). Geoheritage, 10(3), 393-403.

Castanera, D., Silva, B. C., Santos, V. F., Malafaia, E., & Belvedere, M. (2020). Tracking Late Jurassic ornithopods in the Lusitanian Basin of Portugal: ichnotaxonomic implications. Acta Palaeontologica Polonica, 65(2), 399-412.

Castanera, D., Malafaia, E., Silva, B. C., Santos, V. F., & Belvedere, M. (2021). New dinosaur, crocodylomorph and swim tracks from the Late Jurassic of the Lusitanian Basin: implications for ichnodiversity. Lethaia, 54 (2), 271-287.

Castanera, D., Bádenas, B., Aurell, M., Canudo, J. I., & Gasca, J. M. (2022). New ornithopod tracks from the Lower Cretaceous El Castellar Formation (Spain): Implications for track preservation and evolution of ornithopod footprints. Palaeogeography, Palaeoclimatology, Palaeoecology, 591, 110866.

Campos Soto, S., Benito, M. I., Mas, R., Caus, E., Cobos, A., Suárez González, P., & Quijada Van Den Berghe, I. E. (2019). Revisiting the Late Jurassic-Early Cretaceous of the NW South Iberian Basin: new ages and sedimentary environments. Journal of Iberian Geology 45, 471–510.

Canudo, J. I., Ruiz-Omeñaca, J. I., Aurell, M., Barco, J. L., & Cuenca-Bescos, G. (2006). A megatheropod tooth from the late Tithonian-middle Berriasian (Jurassic Cretaceous transition) of Galve (Aragon, NE Spain). Neues Jahrbuch Fur Geologie Und Palaontologie Abhandlungen, 239(3), 77.

Canudo, J. I., Gasca, J. M., Moreno-Azanza, M., & Aurell, M. (2012). New information about the stratigraphic position and age of the sauropod *Aragosaurus ischiaticus* from the Early Cretaceous of the Iberian Peninsula. Geological Magazine, 149(2), 252-263.

Cobos, A., Lockley, M. G., Gascó, F., Royo–Torres, R., & Alcalá, L. (2014). Megatheropods as apex predators in the typically Jurassic ecosystems of the Villar del Arzobispo Formation (Iberian Range, Spain). Palaeogeography, Palaeoclimatology, Palaeoecology, 399, 31-41.

Cohen, A. S., Halfpenny, J., Lockley, M., & Michel, E. (1993). Modern vertebrate tracks from Lake Manyara, Tanzania and their paleobiological implications. Paleobiology, 19(4), 433-458.

Colbert, E. H., & Merrilees, D. (1967). Cretaceous dinosaur footprints from Western Australia. Journal of the Royal Society of Western Australia, 50(1), 21-25.

Cuenca-Bescós, G., Ezquerra, R., Pérez, F., Soria, A.R. 1993. Las huellas de dinosaurios (icnitas) de Los Corrales del Pelejón. Gobierno de Aragón. Departamento de Cultura y Educación, 14pp.

Díaz-Martínez, I., Pereda-Suberbiola, X., Perez-Lorente, F., & Canudo, J. I. (2015). Ichnotaxonomic review of large ornithopod dinosaur tracks: temporal and geographic implications. PloS one, 10(2), e0115477.

Dietrich, O.W. 1927. Über Fährten ornithopodider Saurier im Oberkirchner Sandstein. Zeitschrift der Deutschen Geologischen Gesellschaft, 78, 614-621

Falkingham, P. L., Bates, K. T., Avanzini, M., Bennett, M., Bordy, E. M., Breithaupt, B. H., ... & Belvedere, M. (2018). A standard protocol for documenting modern and fossil ichnological data. Palaeontology, 61(4), 469-480.

Fanti, F., Contessi, M., Nigarov, A., & Esenov, P. (2013). New data on two large dinosaur tracksites from the Upper Jurassic of Eastern Turkmenistan (Central Asia). Ichnos, 20(2), 54-71.

Fuentes Vidarte, C., & Meijide Calvo, M. (1998). Icnitas de dinosaurios terópodos en el Weald de Soria (Espana). Nuevo icnogénero *Kalohipus*. *Estudios geológicos*, *54*(3-4), 147-152.

García-Cobeña, J., Cobosa, A., & Verdú, F. J. (2023). Ornithopod tracks and bones: Paleoecology and an unusual evidence of quadrupedal locomotion in the Lower Cretaceous of eastern Iberia (Teruel, Spain). Cretaceous Research, 105473.

García-Ramos, J.C. 1977. Hallazgo de huellas de dinosaurio (Theropoda y Ornithopoda) en la costa asturiana, Asturnatura, 3 (3-4), 171-172.

García-Ortiz, E., & Pérez-Lorente, F. (2014). Palaeoecological inferences about dinosaur gregarious behaviour based on the study of tracksites from La Rioja area in the Cameros Basin (Lower Cretaceous, Spain). Journal of Iberian Geology, 40(1), 113.

Gasca, J. M., Moreno-Azanza, M., Bádenas, B., Díaz-Martínez, I., Castanera, D., Canudo, J. I., & Aurell, M. (2017). Integrated overview of the vertebrate fossil record of the Ladruñán anticline (Spain): evidence of a Barremian alluvial-lacustrine system in NE Iberia frequented by dinosaurs. Palaeogeography, Palaeoclimatology, Palaeoecology, 472, 192-202.

Gascó, F., Cobos, A., Royo-Torres, R., Mampel, L., & Alcalá, L. (2012). Theropod teeth diversity from the Villar del Arzobispo Formation (Tithonian–Berriasian) at Riodeva (Teruel, Spain). *Palaeobiodiversity and Palaeoenvironments*, *92*(2), 273-285.

Getty, P. R., Aucoin, C., Fox, N., Judge, A., Hardy, L., & Bush, A. M. (2017). Perennial lakes as an environmental control on theropod movement in the Jurassic of the Hartford Basin. Geosciences, 7(1), 13.

Gierlinski, G. D., Niedzwiedzki, G., & Nowacki, P. (2009). Small theropod and ornithopod footprints in the Late Jurassic of Poland. Acta Geologica Polonica, 59(2), 221-234.

Heredia, A. M., Díaz-Martínez, I., Pazos, P. J., Comerio, M., & Fernández, D. E. (2020). Gregarious behaviour among non-avian theropods inferred from trackways: A case study from the Cretaceous (Cenomanian) Candeleros Formation of Patagonia, Argentina. Palaeogeography, Palaeoclimatology, Palaeoecology, 538, 109480.

Hernández Medrano, N., Pascual Arribas, C., Latorre Macarrón, P., & Sanz Pérez, E. (2008). Contribución de los yacimientos de icnitas sorianos al registro general de Cameros. Zubía, (23), 79-120.

Hitchcock, E. (1845). An attempt to name, classify, and describe the animals that made the fossil footmarks of New England. In *Proceedings of the 6th Annual Meeting of the*

Association of American Geologists and Naturalists, New Haven, Connecticut (Vol. 6, pp. 23-25).

Hornung, J. J., Böhme, A., van der Lubbe, T., Reich, M., & Richter, A. (2012). Vertebrate tracksites in the Obernkirchen Sandstone (late Berriasian, Early Cretaceous) of northwest Germany—their stratigraphical, palaeogeographical, palaeoecological, and historical context. Paläontologische Zeitschrift, 86(3), 231-267.

Hornung, J. J., Böhme, A., Schlüter, N., & Reich, M. (2016). Diversity, ontogeny, or both? A morphometric approach to iguanodontian ornithopod (Dinosauria: ornithischia) track assemblages from the Berriasian (Lower Cretaceous) of North Western Germany. Dinosaur Tracks. The Next Steps, 202-225.

Kuhn, O. (1958). Die fahrten der vorzeitlichen Amphibien und reptilien. Verlagshaus Meisenbach, Bamberg, 64p.

Li, J. (2011). On the dinosaur tracks from the Lower Cretaceous of Otog Qi, Inner Mongolia. China Press

Li, Y., Jiang, S., & Wang, X. (2020). The largest species of *Asianopodus* footprints from Junggar Basin, Xinjiang, China. Chinese Science Bulletin, 65(18), 1875-1887.

Lockley, M. G. (1991). *Tracking dinosaurs: a new look at an ancient world*. Cambridge University Press

Lockley, M. G. (2009). New perspectives on morphological variation in tridactyl footprints: clues to widespread convergence in developmental dynamics. Geological Quarterly, 53(4), 415-432.

Lockley, M. G., Houck, K. J., & Prince, N. K. (1986). North America's largest dinosaur trackway site: Implications for Morrison Formation paleoecology. Geological Society of America Bulletin, 97(10), 1163-1176.

Lockley, M. G., Meyer, C. A., & Santos, V. F. (1996). *Megalosauripus*, *Megalosauropus* and the concept of megalosaur footprints. In: The Continental Jurassic: Symposium Volume: Museum of Northern Arizona Bulletin (Vol. 60, pp. 113-118).

Lockley, M. G., Meyer, C. A., & Santos, V. F. (2000). *Megalosauripus* and the problematic concept of megalosaur footprints. Gaia, 15, 313-337.

Lockley, M. G., Breithaupt, B. H., Matthews, N. A., Shibata, K., & Hunt-Foster, R. (2021). A preliminary report on an Early Jurassic *Eubrontes*-dominated tracksite in the Navajo Sandstone formation at the mail station dinosaur tracksite, San Juan County, Utah. Bull. NM Mus. Nat. Hist. Sci, 82, 195-208.

Lucas, S. G., Klein, H., Lockley, M. G., Spielmann, J. A., Gierlinski, G. D., Hunt, A. P., & Tanner, L. H. (2006). Triassic-Jurassic stratigraphic distribution of the theropod footprint ichnogenus *Eubrontes*. New Mexico Museum of Natural History and Science Bulletin, 37, 86-93.

Lull, R.S., 1904. Fossil footprints of the Jura-Trias of North America. Memoirs of the Boston Society of Natural History 5, 461e557.

Marchetti, L., Belvedere, M., Voigt, S., Klein, H., Castanera, D., Díaz-Martínez, I., ... & Farlow, J. O. (2019). Defining the morphological quality of fossil footprints. Problems and principles of preservation in tetrapod ichnology with examples from the Palaeozoic to the present. Earth-Science Reviews, 193, 109-145.

Martín-Chivelet, J., López-Gómez, J., Aguado, R., Arias, C., Arribas, J., Arribas, M.E., Aurell, M., Bádenas, B., Benito, M.I., Bover-Arnal, T., Casas-Sainz, A., Castro, J.M., Coruña, F., de Gea, G.A., Fornós, J.J., Fregenal-Martínez, M., García-Senz, J., Garófano, D., Gelabert, B., Giménez, J., González-Acebrón, J., Guimerà, J., Liesa, C. L., Mas, R., Meléndez, N., Molina, J.M., Muñoz, J.A., Navarrete, R., Nebot, M., Nieto, L.M., Omodeo-Salé, S., Pedrera, A., Peropadre, C., Quijada, I.E., Quijano, M.L., Reolid, M., Robador, A., Rodríguez-López, J.P., Rodríguez-Perea, A., Rosales, I., Ruiz-Ortiz, P.A., Sàbat, F., Salas, R., Soria, A.R., Suarez-Gonzalez, P., Vilas, L., 2019. The late Jurassic–early cretaceous rifting. In: Quesada, C., Oliveira, J.T. (Eds.), The Geology of Iberia: A Geodynamic Approach, The Alpine Cycle, Volume 3. Springer, Heidelberg, pp. 170–250.

Marty, D. 2008. Sedimentology, taphonomy, and ichnology of Late Jurassic dinosaur tracks from the Jura carbonate platform (Chevenez-Combe Ronde tracksite, NW Switzerland): insights into the tidal-flat palaeoenvironment and dinosaur diversity, locomotion, and palaeoecology. GeoFocus 21: 1–278.

Marty, D., Belvedere, M., Razzolini, N. L., Lockley, M. G., Paratte, G., Cattin, M., ... & Meyer, C. A. (2018). The tracks of giant theropods (*Jurabrontes curtedulensis* ichnogen. & ichnosp. nov.) from the Late Jurassic of NW Switzerland: palaeoecological & palaeogeographical implications. *Historical Biology*, *30*(7), 928-956.

Mas, R., Alonso, A., Meléndez, N. (1984). La formación Villar del Arzobispo: un ejemplo de llanuras de mareas siliciclásticas asociadas a plataformas carbonatadas. Jurasico terminal (NW de Valencia y E de Cuenca). Publicaciones de Geología 20, 175–188.

Matsukawa, M., Shibata, K., Kukihara, R., Koarai, K., & Lockley, M. G. (2005). Review of Japanese dinosaur track localities: implications for ichnotaxonomy, paleogeography and stratigraphic correlation. Ichnos, 12(3), 201-222.

Melchor, R. N., Genise, J. F., Buatois, L. A., & Umazano, A. M. (2012). Fluvial environments. In: *Developments in Sedimentology*, Trace Fossils as Indicators of Sedimentary Environments *64*, 329-378.

Melchor, R. N., Rivarola, D. L., Umazano, A. M., Moyano, M. N., & Belmontes, F. R. M. (2019). Elusive Cretaceous Gondwanan theropods: the footprint evidence from central Argentina. Cretaceous Research, 97, 125-142.

Meyer, C. A., Belvedere, M., Englich, B., & Lockley, M. G. (2021). A reevaluation of the Late Jurassic dinosaur tracksite Barkhausen (Wiehengebirge, Northern Germany). PalZ, 95(3), 537-558.

Milner, A. C. (2002). Theropod dinosaurs of the Purbeck limestone group, Southern England. Special Papers in Palaeontology, 68, 191-202.

Moratalla, J. J., & Hernán, J. (2010). Probable palaeogeographic influences of the Lower Cretaceous Iberian rifting phase in the Eastern Cameros Basin (Spain) on dinosaur trackway orientations. Palaeogeography, palaeoclimatology, palaeoecology, 295(1-2), 116-130.

Navarro-Lorbés, P., Ruiz, J., Díaz-Martínez, I., Isasmendi, E., Sáez-Benito, P., Viera, L., ... & Torices, A. (2021). Fast-running theropods tracks from the Early Cretaceous of La Rioja, Spain. Scientific Reports, 11(1), 23095.

von Nopcsa, F. (1923). Die Familien der Reptilien. *Fortschritte der Geol und Paläontologie*, *2*, 1-210.

Olsen, P. E., Smith, J. B., & McDonald, N. G. (1998). Type material of the type species of the classic theropod footprint genera *Eubrontes*, *Anchisauripus*, and *Grallator* (Early Jurassic, Hartford and Deerfield basins, Connecticut and Massachusetts, USA). Journal of vertebrate Paleontology, 18(3), 586-601.

Ostrom, J. H. (1972). Were some dinosaurs gregarious?. Palaeogeography, Palaeoclimatology, Palaeoecology, 11(4), 287-301.

Pereda Suberbiola,. X, Galton,.PM, Ruiz Omeñaca. J., & Canudo, J. I. (2005). Dermal spines of stegosaurian dinosaurs from the Lower Cretaceous (Hauterivian-Barremian) of Galve (Teruel, Aragon, Spain). Geogaceta, 38, 35-38.

Pérez-Lorente, F. (2009). Las huellas de Galve. Instituto de Estudios Turolenses, editors. II Jornadas paleontológicas de Galve. Homenaje a José María Herrero, 85-114.

Pérez-Lorente, F. (2015). Dinosaur footprints & trackways of La Rioja. Indiana University Press.

Perron, J.T., Myrow, P.M., Huppert, K.L., Koss, A.R., Wickert, A.D., 2018. Ancient record of changing flows from wave ripple defects. *Geology*, 46, 10, 875–878.

Piñuela Suárez, L. (2015). Huellas de dinosaurios y otros reptiles del Jurásico Superior de Asturias. PhD Thesis.

Piñuela, L., García-Ramos, J. C., Romano, M., & Ruiz-Omenaca, J. I. (2016). First record of gregarious behavior in robust medium-sized Jurassic Ornithopods: evidence from the Kimmeridgian trackways of Asturias (N. Spain) and some general considerations on other medium-large ornithopod tracks in the Mesozoic record. Ichnos, 23(3-4), 298-311.

Pouech, J., Amiot, R., Lecuyer, C., Mazin, J. M., Martineau, F., & Fourel, F. (2014). Oxygen isotope composition of vertebrate phosphates from Cherves-de-Cognac (Berriasian, France): environmental and ecological significance. Palaeogeography, Palaeoclimatology, Palaeoecology, 410, 290-299.

Rauhut, O. W., Pinuela, L., Castanera, D., Garcia-Ramos, J. C., & Cela, I. S. (2018). The largest European theropod dinosaurs: remains of a gigantic megalosaurid and giant theropod tracks from the Kimmeridgian of Asturias, Spain. PeerJ, 6, e4963.

Razzolini, N. L., Oms, O., Castanera, D., Vila, B., Dos Santos, V. F., & Galobart, À. (2016). Ichnological evidence of megalosaurid dinosaurs crossing Middle Jurassic tidal flats. Scientific reports, 6(1), 1-15.

Razzolini, N. L., Belvedere, M., Marty, D., Paratte, G., Lovis, C., Cattin, M., & Meyer, C. A. (2017). *Megalosauripus transjuranicus* ichnosp. nov. A new Late Jurassic theropod ichnotaxon from NW Switzerland and implications for tridactyl dinosaur ichnology and ichnotaxomy. Plos one, 12(7), e0180289.

Richter, A. Böhme, A. (2016). Too Many Tracks: Preliminary Description and Interpretation of the Diverse and Heavily Dinoturbated Early Cretaceous "Chicken Yard" Ichnoassemblage (Obernkirchen Tracksite, Northern Germany). In: *Dinosaur Tracks: The Next Steps*, 334-357.

Royo-Torres, R., Upchurch, P., Mannion, P. D., Mas, R., Cobos, A., Gascó, F., ... & Sanz, J. L. (2014). The anatomy, phylogenetic relationships, and stratigraphic position of the Tithonian–Berriasian Spanish sauropod dinosaur *Aragosaurus ischiaticus*. Zoological Journal of the Linnean Society, 171(3), 623-655.

Ruiz, J., & Torices, A. (2013). Humans running at stadiums and beaches and the accuracy of speed estimations from fossil trackways. Ichnos, 20(1), 31-35.

Ruiz-Omeñaca, J. I., Canudo, J. I., Aurell, M., Bádenas, B., Barco, J. L., Cuenca-Bescós, G., & Ipas, J. (2004). Estado de las investigaciones sobre los vertebrados del Jurásico Superior y Cretácico Inferior de Galve (Teruel). Estudios geológicos, 60(3-6), 179-202.

Sánchez-Fenollosa, S., Verdú, F. J., Suñer, M., & de Santisteban, C. (2022). Tracing Late Jurassic ornithopod diversity in the eastern Iberian Peninsula: *Camptosaurus*-like postcranial remains from Alpuente (Valencia, Spain). Journal of Iberian Geology, 48(1), 65-78.

Sánchez-Fenollosa, S., Verdú, F. J., Cobos, A. (2023). The largest ornithopod (Dinosauria: Ornithischia) from the Upper Jurassic of Europe sheds light on the evolutionary history of basal ankylopollexians, Zoological Journal of the Linnean Society. https://doi.org/10.1093/zoolinnean/zlad076

Santos, A. A., Villanueva-Amadoz, U., Royo-Torres, R., Sender, L. M., Cobos, A., Alcala, L., & Diez, J. B. (2018). Palaeobotanical records associated with the first dinosaur defined in Spain: Palynostratigraphy, taxonomy and palaeoenvironmental remarks. Cretaceous Research, 90, 318-334.

Sanz, J. L., Buscalioni, A. D., Casanovas, M. L., & Santafé, J. V. (1987). Dinosaurios del Cretácico Inferior de Galve (Teruel, España). Estudios geológicos, 43(Extra), 45-64.

Sarjeant, W. A., Delair, J. B., & Lockley, M. G. (1998). The footprints of *Iguanodon*: a history and taxonomic study. Ichnos: An International Journal of Plant & Animal, 6(3), 183-202.

Shillito, A. P., & Davies, N. S. (2019). Dinosaur-landscape interactions at a diverse Early Cretaceous tracksite (Lee Ness Sandstone, Ashdown Formation, southern England). Palaeogeography, Palaeoclimatology, Palaeoecology, 514, 593-612.

Torcida Fernández-Baldor, F., Díaz-Martínez, I., Huerta, P., Montero Huerta, D., & Castanera, D. (2021). Enigmatic tracks of solitary sauropods roaming an extensive lacustrine megatracksite in Iberia. Scientific reports, 11(1), 1-17.

Turmine-Juhel, P., Wilks, R., Brockhurst, D., Austen, P. A., Duffin, C. J., & Benton, M. J. (2019). Microvertebrates from the Wadhurst Clay Formation (Lower Cretaceous) of Ashdown Brickworks, East Sussex, UK. Proceedings of the Geologists' Association, 130(6), 752-769.

Thulborn, T. (1990). Dinosaur tracks. Chapman and Hall. 410p.

Xing, L. D., Niedźwiedzki, G., Lockley, M. G., Zhang, J. P., Cai, X. F., Persons IV, W. S., & Ye, Y. (2014). *Asianopodus*-type footprints from the Hekou Group of Honggu District, Lanzhou City, Gansu, China and the “heel” of large theropod tracks. Palaeoworld, 23(3-4), 304-313.

Xing, L., Lockley, M. G., Yang, G., Cao, J., McCrea, R. T., Klein, H., ... & Dai, H. (2016). A diversified vertebrate ichnite fauna from the Feitianshan Formation (Lower Cretaceous) of southwestern Sichuan, China. Cretaceous Research, 57, 79-89.

Xing, L. D., Lockley, M. G., Klein, H., Zhang, L. J., Romilio, A., Scott Persons, W., ... & Wang, M. Y. (2021a). The new ichnotaxon *Eubrontes nobitai* ichnosp. nov. and other saurischian tracks from the Lower Cretaceous of Sichuan Province and a review of Chinese *Eubrontes*-type tracks. Journal of Palaeogeography, 10, 1-19.

Xing, L., Lockley, M. G., Jia, C., Klein, H., Niu, K., Zhang, L., ... & Wang, M. (2021b). Lower cretaceous avian-dominated, theropod, thyreophoran, pterosaur and turtle track assemblages from the Tugulu Group, Xinjiang, China: ichnotaxonomy and palaeoecology. PeerJ, 9, e11476.

Xing, L., Lockley, M. G., Mao, Z., Klein, H., Gu, Z., Bai, C., ... & Wan, X. (2021c). A new dinosaur track site from the earliest Cretaceous (Berriasian) part of the Tuchengzi Formation, Hebei Province, China: Implications for morphology, ontogeny and paleocommunity structure. *Palaeogeography, Palaeoclimatology, Palaeoecology*, *580*, 110619.

Figure captions

Figure 1: Geographical and geological setting of the *Los Corrales del Pelejón* tracksite. A) Orthophoto showing the distribution of the lithostratigraphic units outcropping in the Galve syncline. B) Geological setting of the Maestrazgo Basin in northeast Spain showing the distribution of the sub-basins (modified from Martín-Chivelet et al., 2019). C) Synthetic log showing the stratigraphy (based on Aurell et al., 2016, 2019) of the Galve sub-basin.

Figure 2: Stratigraphic and sedimentological analysis of the lower part of the Galve Fm in the studied area. A) Facies distribution and correlation between the *Pelejón* and *Los Corrales del Pelejón* sections, indicating the sandstone packages G1 to G7 used as reference levels for lateral correlation. Note the normal fault controlling sedimentation in the lowermost part (see packages G1 to G3) and the location of the *Los Corrales del Pelejón* tracksite in sandstone package G6. B) Paleoenvironmental interpretation of the studied successions and the broader-scale sedimentary context in the Galve sub-basin. The location of the *Los Corrales del Pelejón* tracksite and paleocurrent data from different facies are indicated in the paleoenvironmental scheme (see also Supplementary data S1 and S2).

Figure 3: Sedimentological context of the *Los Corrales del Pelejón* tracksite beds. A) Detailed log of the tracksite beds, indicating the four sedimentary layers where the dinosaur tracks are preserved. B-C) Outcropping layers in the tracksite in the different sectors. Note that mainly layer 1 is outcropping in Sector B due to current erosion (see also log in A), whereas layers 1 to 4 crop out in Sector A. Nevertheless, in the upper area of Sector A, the ripples in layers 2 and 3 disappear laterally, so that these layers are laterally equivalent to the uppermost layer 1 in this sector (see Fig. 3A). Notice peaked- and rounded-crest wave ripples in layers 2 and 3, respectively, and the tracks of trackways CP1 and CP2 on layers 4 and 1, parallel to the ripple crests. D) Detailed

picture of C. Note the invertebrate traces on layers 3 and 4 and the lateral disappearance of rippled layer 3 (see also log in A). E) Detailed picture of the upper area of Sector A.

Figure 4: Tracks and trackways of the *Los Corrales del Pelejón* tracksite. A) Solid three-dimensional model (obtained with ParaView) of the surface of the tracksite. B) Sketch map of the tracksite. Note that the tracks have been numbered consecutively, including missing tracks. Note also that the sketch map in B has not been directly drawn from A. C) Historic picture taken in 1992 of track CP1.4. D) Rose diagram showing the orientation of the midline of the trackways CP1-CP7. Note that the orientations of the trackways represented in the diagram have been measured from the map.

Figure 5: Dinosaur tracks of high morphological quality from the *Los Corrales del Pelejón* tracksite. *Megalosauripus* cf. *transjuranicus* (A-J), Grallatoridae indet. (K), cf. *Iguanodontipus* isp. (L). A) CP1.1. B) CP1.4. C) CP2.2. D) CP2.4. E) CP3.3. F) CP3.7. G) CP5.1. H) CP5.3. I) CP6.4. J) CP9. K) CP4.2. L) CP7.4. Scale bars = 15 cm (K), 25 cm (A, B, F, J), 30 cm (E, G, H, L), 35 cm (C, D, I).

Figure 6*:* A) *Eubrontes giganteus* Hitchcock, 1845 (redrawn from Olsen et al., 1998); B) *Eutynichnium lusitanicum* Nopcsa, 1923 (redrawn from Lockley et al., 2000); C) *Megalosauropus broomensis* (Colbert and Merrilees, 1967); D) *Bueckeburgichnus maximus* (redrawn from Lockley, 2000); E) *Eubrontes nobitai* (redrawn from Xing et al., 2021a); F) *Megalosauripus uzbekistanicus* (redrawn from Lockley et al., 1996); G) *Megalosauripus transjuranicus* (redrawn from Razzolini et al., 2017); H) *Jurabrontes curtedulensis* (redrawn from Marty et al., 2018); I) *Iberosauripus grandis* (redrawn from Cobos et al., 2014); J) *Asianopodus pulvinicalx* (redrawn from Matsukawa et al., 2005); K) *Asianopodus robustus* (redrawn from Xing et al., 2021b); L) *Asianopodus niui* (redrawn from Xing et al., 2021b); M) *Asianopodus wangi* (redrawn from Xing et al., 2021c); N) CP1.1; O) CP1.4; P) CP2.4; Q) CP3.7; R) *Grallator* isp. from the Late Jurassic of Asturias (redrawn from Castanera et al., 2016b); S) *Kalohipus bretunensis* from the Berriasian of Spain (redrawn from Castanera et al., 2015, after Fuentes Vidarte and Meijide Calvo, 1998); T) *Iguanodontipus burreyi* (holotype, redrawn from Sarjeant et al., 1998); U) *Iguanodontipus burreyi* (previously *Wealdenichnites iguanodontoides*) (redrawn from Díaz-Martínez et al., 2015, after Dietrich, 1927); V) *Iguanodontipus burreyi* (previously *Iguanodontipus? oncalensis*) (redrawn from Castanera et al., 2013);

W) unnamed ornithopod track from the Late Jurassic of Asturias (redrawn from Piñuela et al., 2016); X) Iguanodontipodidae from the Late Jurassic of Portugal (redrawn from Castanera et al., 2020); Y) CP7.4. Scale bars = 10 cm (A-Q), 5 cm (R-S).

Table 1: Measurements of the dinosaur tracks of the *Los Corrales del Pelejón* tracksite. MP, Morphological preservation value (following Marchetti et al., 2019); FL, footprint length; FW, footprint width; FL/FW, footprint length/footprint width ratio; LII, LIII, LIV, digit total length (from the tip to the heel pad impression); DIII, digit III length excluding the heel pad; WII, WIII, WIV, digit width; HPL, heel pad length; HPW, heel pad width. II^III, III^IV, II^IV, interdigital divarication angles; ATl, anterior triangle length; ATw, anterior triangle width; AT ratio (ATl/ATw (mesaxony). FL, FW, LII, LIII, LIV, DIII, WII, WIII, WIV, HPL, HPW, ATl, ATw, in cm. II^III, III^IV, II^IV in degrees (◦). NP, not preserved. NM, not measured due to poor preservation. ? denotes uncertainty in the measurement.

Supplementary data

S1: Facies description and interpretation of red to ocherish mudstones, gray mudstones, and laminated and/or bioturbated sandstones. The stratigraphic location of sandstone packages (e.g., G4, G5, etc.), paleocurrent data, and the paleoenvironmental scheme are shown in Fig. 2 of the main text. Grain size results are in Supplementary data S3.

S2: Facies description and interpretation of cross-bedded sandstones and poorly bedded conglomerates. The stratigraphic location of sandstone packages (G5, G7 in A), paleocurrent data, and the paleoenvironmental scheme are shown in Fig. 2 of the main text. Grain size results are in Supplementary data S3.

S3: Grain size analysis of muddy and sandy facies of the lower part of the Galve Fm in the *Corrales del Pelejón* section, including the data from beds 1, 3 and 4 of the *Los Correles del Pelejón* tracksite. For the location of samples and beds see Figs. 2A and 3 of the main text.

S4: Bivariate graph plotting the footprint length/footprint width ratio against the mesaxony of the studied tracks with some of the main tridactyl theropod ichnotaxa mentioned in the text. Data taken from Lockley et al. (2021), Xing et al. (2021a), Castanera et al. (2021) and references therein.

Table S1: Measurements of the dinosaur trackways. Orientation of the trackway. PLh, pace length measured from the heel pad impression; PLt, pace length measured from the tip of DIII; SLh, stride length measured from the heel pad impression; SLt, stride length measured from the tip of DIII; FL, footprint length; h, height to the acetabulum; speed following the Alexander (1976) and Ruiz and Torices (2013) formulas. All measurements in meters.

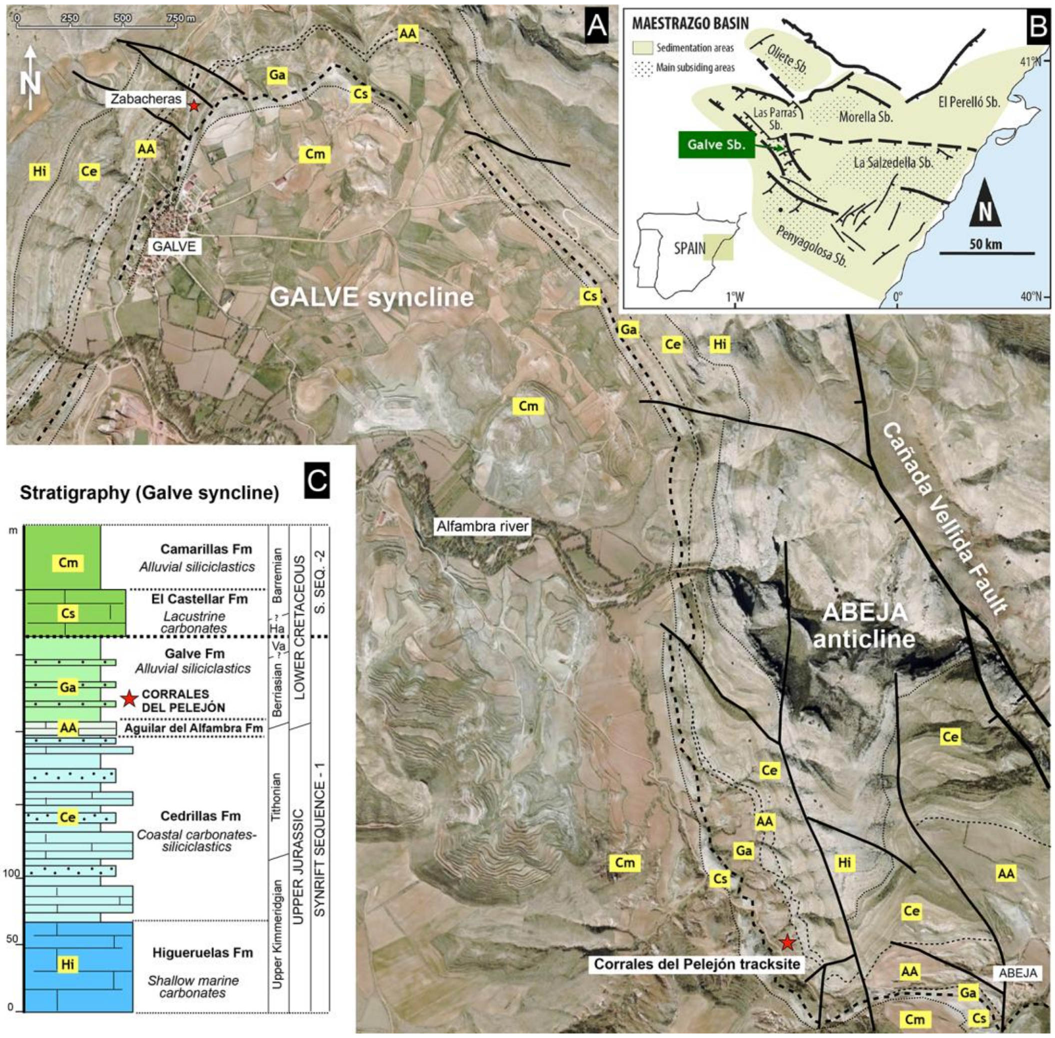

Figure 1

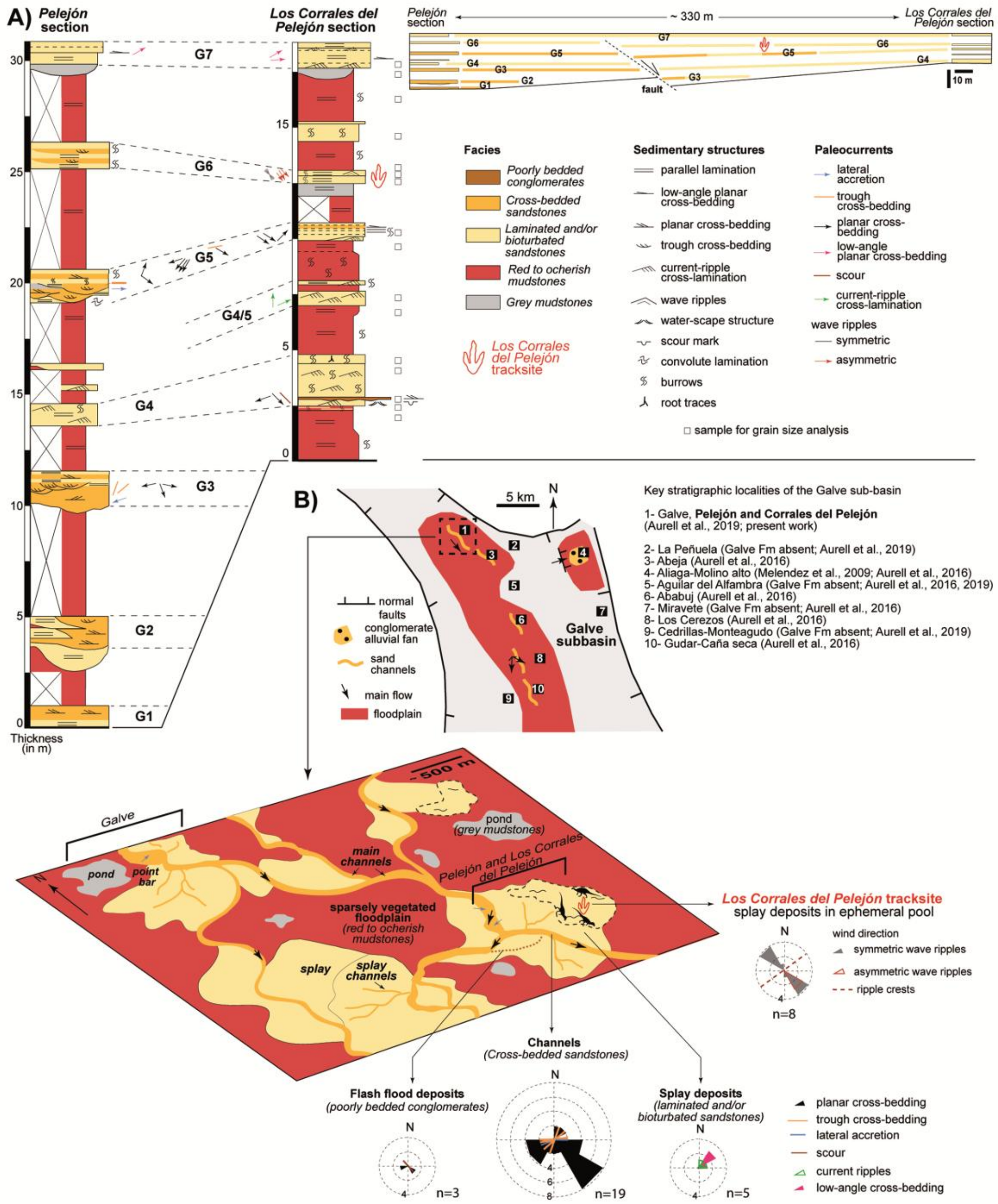
A) Pelejón section
Los Corrales del Pelejón section
G7
G6
G5
G4/5
G4
G3
G2
G1
Thickness (in m)
Pelejón section
~ 330 m
Los Corrales del Pelejón section
fault
10 m
Facies
Poorly bedded conglomerates
Cross-bedded sandstones
Laminated and/or bioturbated sandstones
Red to ocherish mudstones
Grey mudstones
Los Corrales del Pelejón tracksite
Sedimentary structures
parallel lamination
low-angle planar cross-bedding
planar cross-bedding
trough cross-bedding
current-ripple cross-lamination
wave ripples
water-scape structure
scour mark
convolute lamination
burrows
root traces
Paleocurrents
lateral accretion
trough cross-bedding
planar cross-bedding
low-angle planar cross-bedding
scour
current-ripple cross-lamination
wave ripples
symmetric
asymmetric
sample for grain size analysis
B)
5 km
N
Key stratigraphic localities of the Galve sub-basin
1- Galve, Pelejón and Corrales del Pelejón (Aurell et al., 2019; present work)
2- La Peñuela (Galve Fm absent; Aurell et al., 2019)
3- Abeja (Aurell et al., 2016)
4- Aliaga-Molino alto (Melendez et al., 2009; Aurell et al., 2016)
5- Aguilar del Alfambra (Galve Fm absent; Aurell et al., 2016, 2019)
6- Ababuj (Aurell et al., 2016)
7- Miravete (Galve Fm absent; Aurell et al., 2016)
8- Los Cerezos (Aurell et al., 2016)
9- Cedrillas-Monteagudo (Galve Fm absent; Aurell et al., 2019)
10- Gudar-Caña seca (Aurell et al., 2016)
normal faults
conglomerate alluvial fan
sand channels
main flow
floodplain
Galve subbasin
500 m
Galve
pond
point bar
main channels
pond (grey mudstones)
Pelejón and Los Corrales del Pelejón
sparsely vegetated floodplain (red to ocherish mudstones)
splay
splay channels
Los Corrales del Pelejón tracksite
splay deposits in ephemeral pool
wind direction
symmetric wave ripples
asymmetric wave ripples
ripple crests
n=8
Channels (Cross-bedded sandstones)
Flash flood deposits (poorly bedded conglomerates)
Splay deposits (laminated and/or bioturbated sandstones)
n=3
n=19
n=5
planar cross-bedding
trough cross-bedding
lateral accretion
scour
current ripples
low-angle cross-bedding

Figure 2

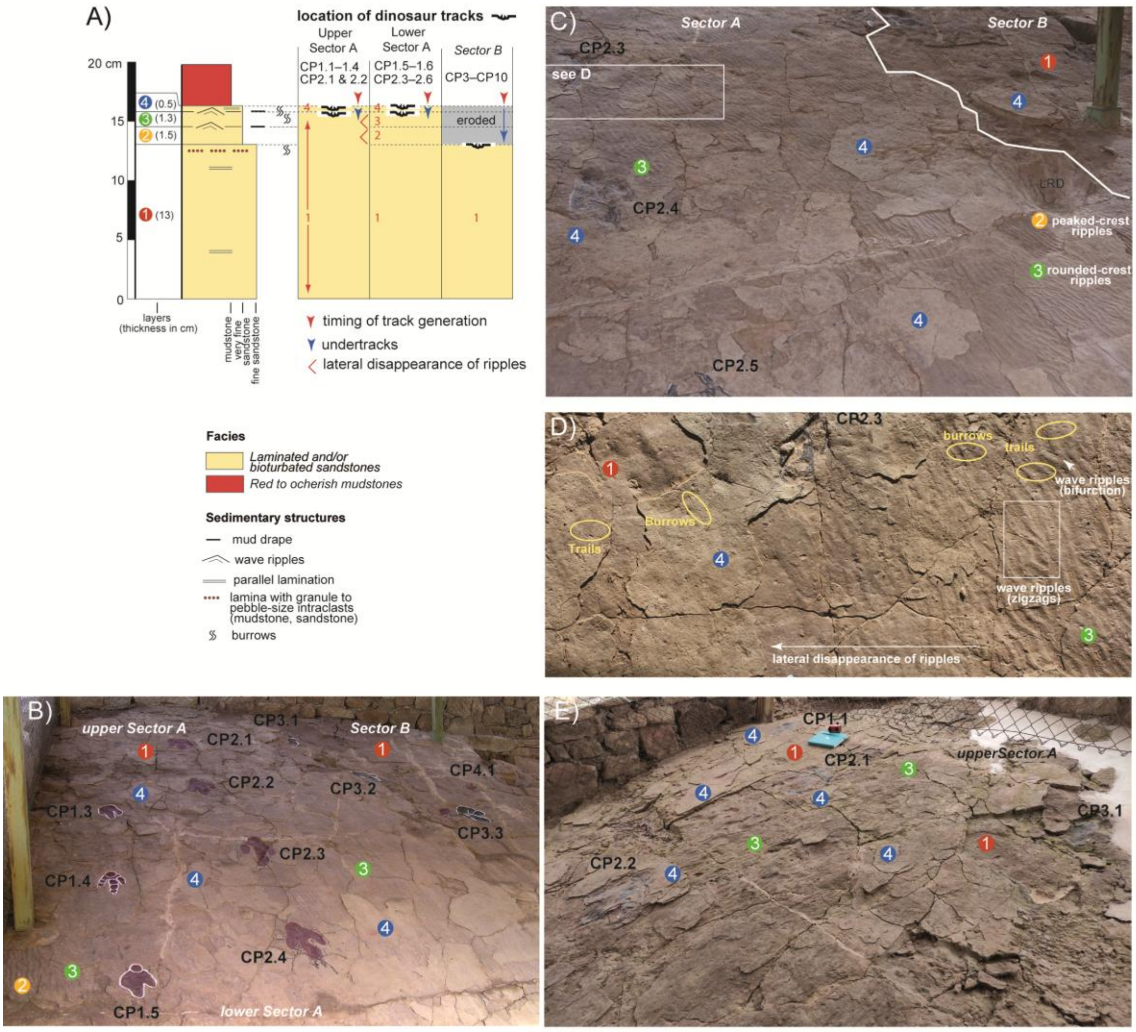
A)
location of dinosaur tracks
Upper Sector A
Lower Sector A
Sector B
CP1.1–1.4
CP2.1 & 2.2
CP1.5–1.6
CP2.3–2.6
CP3–CP10
20 cm
15
10
5
0
(0.5)
(1.3)
(1.5)
(13)
eroded
layers (thickness in cm)
mudstone
very fine sandstone
fine sandstone
timing of track generation
undertracks
lateral disappearance of ripples
Facies
Laminated and/or bioturbated sandstones
Red to ocherish mudstones
Sedimentary structures
mud drape
wave ripples
parallel lamination
lamina with granule to pebble-size intraclasts (mudstone, sandstone)
burrows
C)
Sector A
Sector B
CP2.3
see D
CP2.4
CP2.5
LRD
peaked-crest ripples
rounded-crest ripples
D)
CP2.3
burrows
trails
Trails
Burrows
wave ripples (bifurction)
wave ripples (zigzags)
lateral disappearance of ripples
B)
upper Sector A
Sector B
CP2.1
CP3.1
CP2.2
CP3.2
CP4.1
CP1.3
CP3.3
CP2.3
CP1.4
CP2.4
CP1.5
lower Sector A
E)
CP1.1
CP2.1
upperSector A
CP3.1
CP2.2

Figure 3

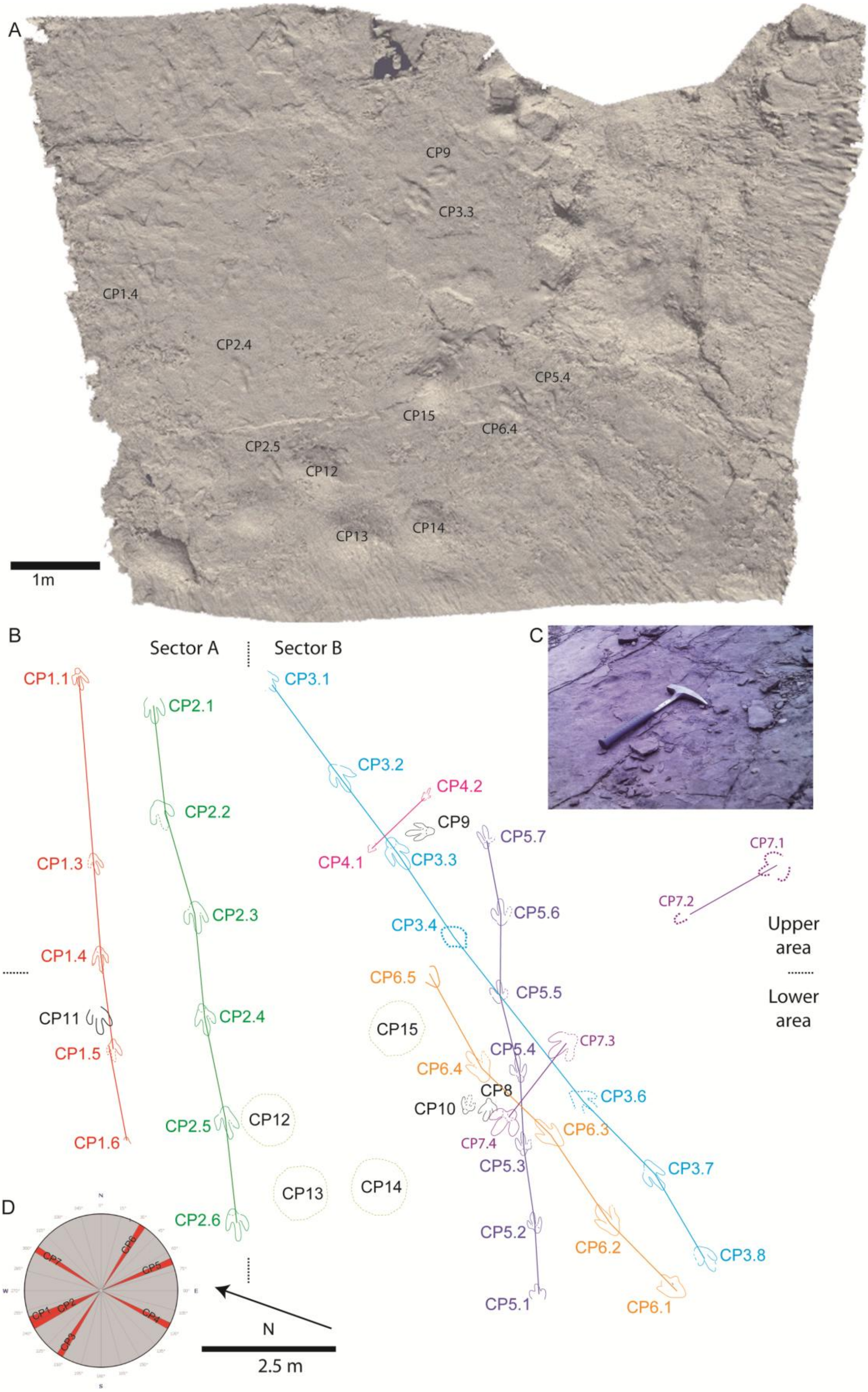
A
CP9
CP3.3
CP1.4
CP2.4
CP5.4
CP15
CP6.4
CP2.5
CP12
CP13
CP14
1m
B
Sector A
Sector B
CP1.1
CP2.1
CP3.1
CP3.2
CP4.2
CP2.2
CP9
CP5.7
CP4.1
CP3.3
CP1.3
CP7.1
CP7.2
CP2.3
CP5.6
CP3.4
Upper area
Lower area
CP1.4
CP6.5
CP5.5
CP11
CP2.4
CP15
CP1.5
CP7.3
CP5.4
CP6.4
CP3.6
CP8
CP10
CP2.5
CP12
CP6.3
CP1.6
CP7.4
CP5.3
CP3.7
CP13
CP14
CP2.6
CP5.2
CP6.2
CP3.8
CP5.1
CP6.1
C
D
N
W
E
S
CP7
CP8
CP5
CP1
CP2
CP4
CP3
N
2.5 m

Figure 4

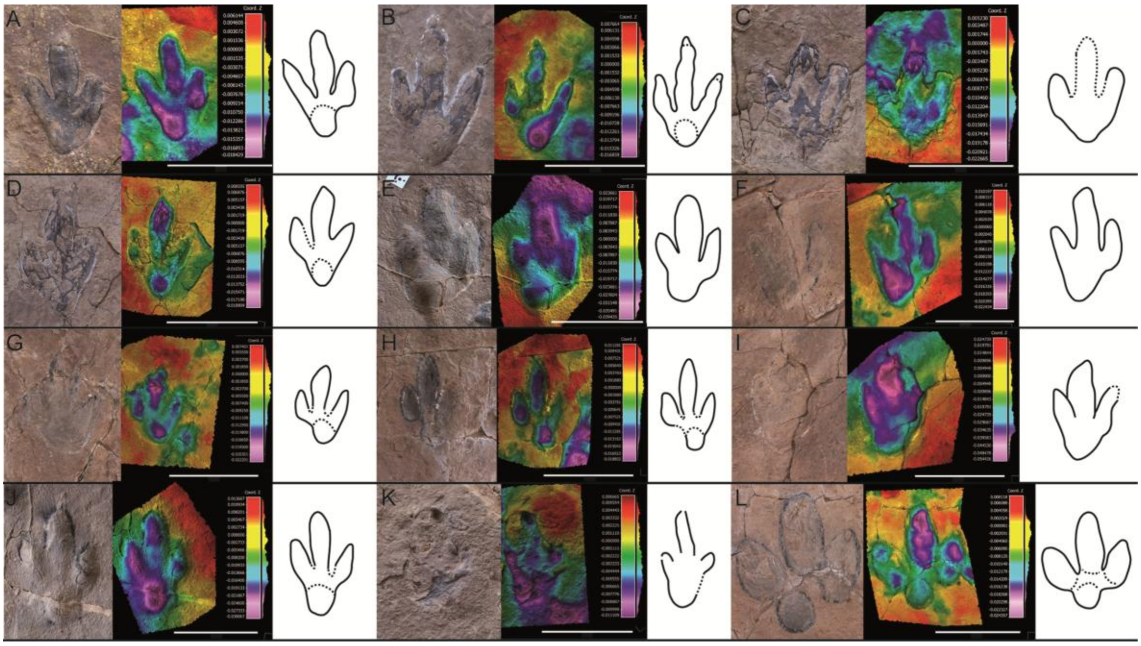

Figure 5

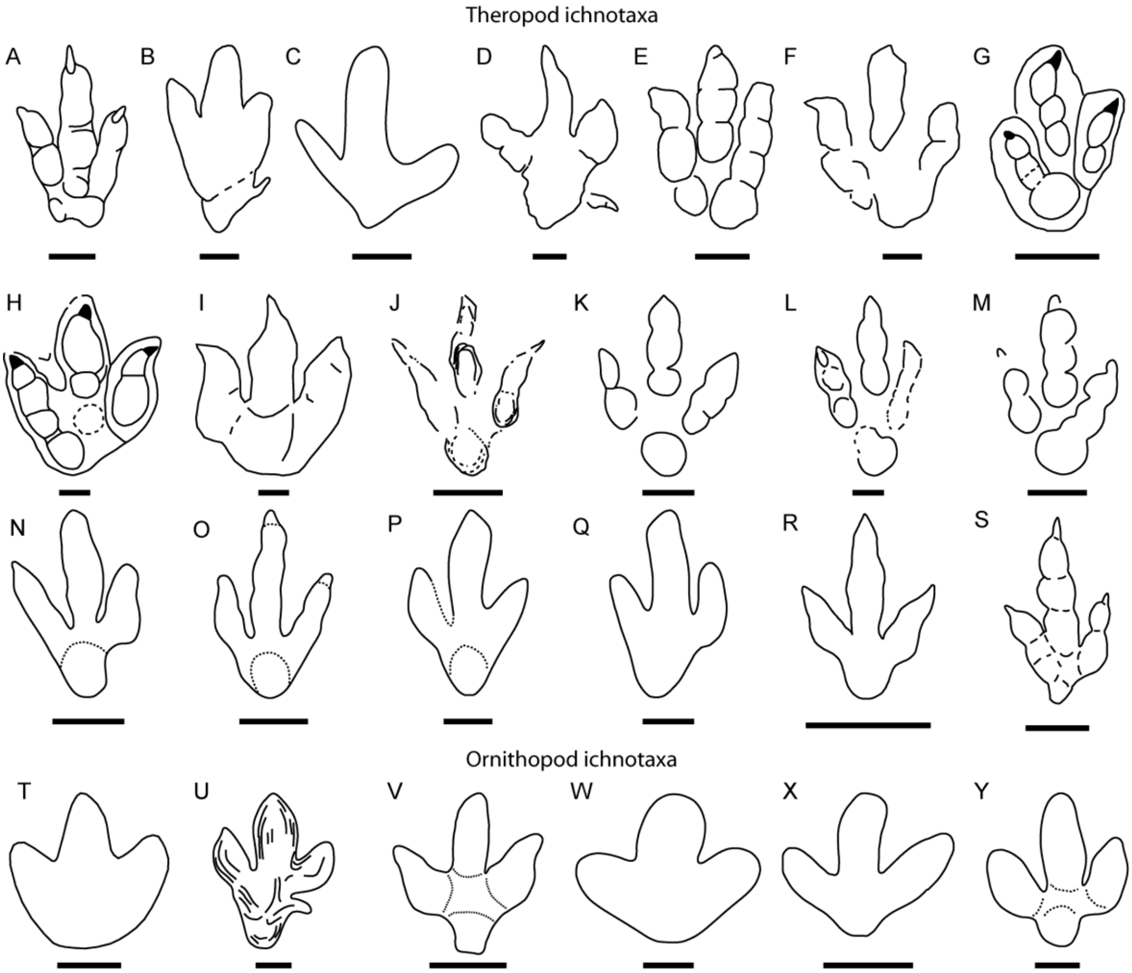

Figure 6

Description		Interpretation
Red to ocherish mudstones		

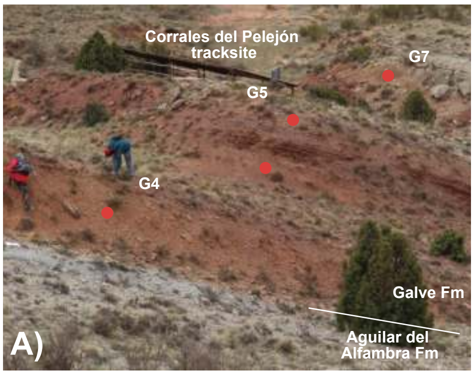

Red to ocherish, locally white, mudstones (see red circles in A) with median grain size of medium silt (see S3), and local intercalated fine sandstones

- mudstones are stratified in laterally extensive tabular beds, a few dm- to 5 m-thick. They are massive or parallel laminated and have local burrows, root traces and mud cracks

- fine sandstones are arranged in parallel or wavy cm-thick laminae

Occurrence: dominant facies

Floodplain fines: unchanneled flows when discharge exceeded the bank-full capacity of the channel network (e.g., Bridge, 2003; Cain and Mountney, 2009):

- mudstones: settling of suspended sediments during waning flows
- fine sandstones: bedload transport under lower-flow regime conditions

Local root traces and mud cracks indicate very local vegetated areas and probably rapid sedimentation preventing soil development and desiccation

Gray mudstones

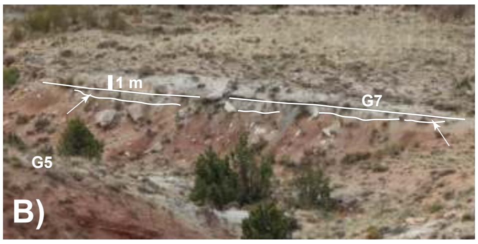

Massive or parallel laminated gray mudstones (see white arrows in B) with median grain size of very fine silt (see S3), arranged in tabular or concave-plane beds, 0.5 m-thick and a few decimeters in lateral extension. Presence of crocodylomorph teeth

Occurrence: very local; underlying laminated and/or bioturbated sandstones

Small ponds in the floodplain with stagnant waters; less likely mud-filled small channels (e.g., Makaske, 2001)

Laminated and/or bioturbated sandstones

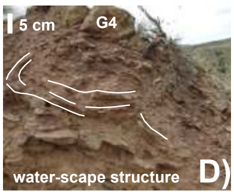

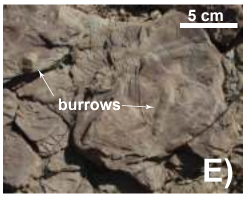

Fine sandstones (median grain size: very fine sand; see S3) stratified in dm-thick beds to 2.5 m-thick bed packages, including:

- Current-ripple cross-laminated sandstones with mud drapes (see C), burrows (see E), and local root traces, and upward-oriented water-scape structures and convolute beds
- parallel-laminated sandstones, occasionally with low-angle planar cross-bedding, associated with the current-ripple cross-laminated beds (see F)
- Massive sandstones, usually burrowed

Occurrence:
- Intercalated and pinching out to red to ocherish mudstones
- Beds with parallel lamination locally observed laterally (attached) to cross-bedded sandstones

Unconfined sheet-like splay deposits emanating from the main fluvial channels (e.g., Burns et al., 2019) or from points where fluvial channels terminated on the alluvial plain (e.g., Tooth, 2000; Cain and Mountney, 2009). Beds laterally (attached) to cross-bedded sandstones would represent levee deposits:

- dominant bedload transport, under upper flow regime (parallel lamination) and low-flow regime (current-ripple cross lamination), and suspended load component (i.e. mud-drapes) (e.g. Hampton and Horton, 2007)
- massive sandstones may represent rapid deposition (e.g., Cain and Mountney, 2009)

Los Corrales del Pelejón **tracksite: see specific description and interpretation in main text**

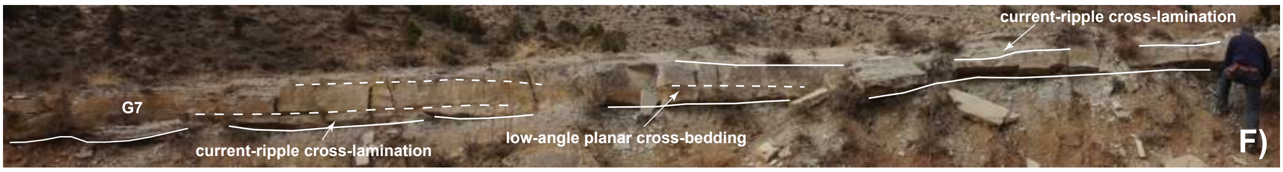

S1. Facies description and interpretation of red to ocherish mudstones, gray mudstones and laminated and/or bioturbated sandstones. Stratigraphic location of sandstone packages (e.g. G4, G5, etc), paleocurrent data and paleoenviornmental scheme are shown in Fig. 2 of main text. Grain size results are in Supplementary data S3.

References:

Bridge, J.S., 2003. Rivers and Floodplains: Forms, Processes, and Sedimentary Record. Wiley-Blackwell, Oxford, UK., 512 p.

Burns, C.E., Mountney, N.P., Hodgson, D.M., Colombera, L., 2019. Stratigraphic architecture and hierarchy of fluvial overbank splay deposits. Journal of the Geological Society 176, 629–649.

Cain, S.A., Mountney, N.P., 2009. Spatial and temporal evolution of a terminal fluvial fan system: the Permian Organ Rock Formation, South-east Utah, USA. Sedimentology 56, 1774–1800.

Hampton, B.A., Norton, B.K., 2007. Sheetflow fluvial processes in a rapidly subsiding basin, Altiplano plateau, Bolivia. Sedimentology 54, 1121–1147.

Makaske, B., 2001. Anastomosing rivers: a review of their classification, origin and sedimentary products. Earth-Science Reviews 53, 149–196.

Tooth, S., 2000. Downstream changes in dryland river channels: the Northern Plains of arid central Australia. Geomorphology 34, 33–54.

Description	Interpretation
Cross-bedded sandstones	
Fine and medium sandstones in m-thick packages, including ribbons (W:T < 15) both isolated and offset stacked and narrow sheets (15 > W:T < 100); (W:T, width-thickness ratio, following Gibling, 2006): - complex internal vertical stacking of planar and trough cross-bedding - lateral accretion surfaces in the *Pelejón* section (Aurell et al., 2016) - local conglomerates at the base Occurrence: - Intercalated in red to ocherish mudstones and changing laterally to laminated and/or bioturbated sandstones (see Fig. 2A in the main text) - locally eroding laminated and/or bioturbated sandstones	**Fluvial channels**: SE-directed main fluvial channels (running roughly parallel to the orientation of the Galve sub-basin) and SW and NE-directed splay channels (see Fig. 2 in the main text)

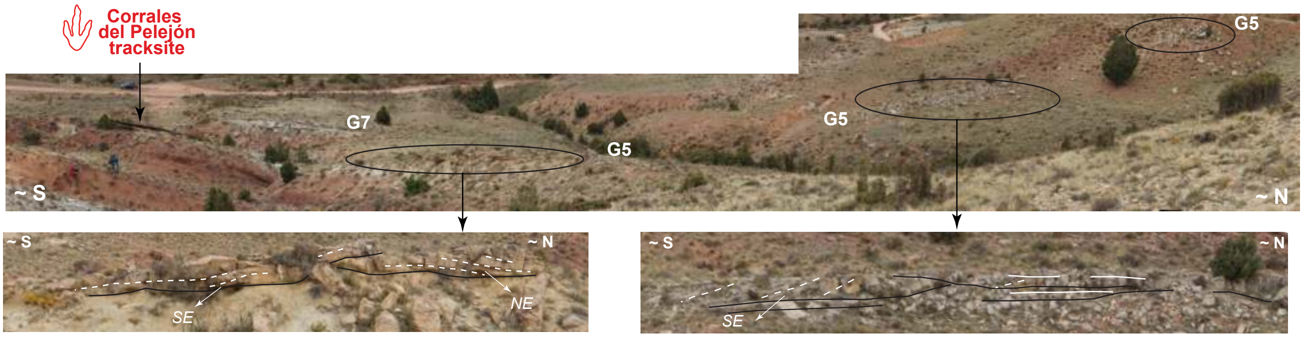

Description		Interpretation
Poorly bedded conglomerates		
	Matrix-supported conglomerates, with coarse sandstone matrix and unsorted subangular to subrounded, granule to pebble-size clasts of limestones (Aguilar del Alfambra Fm), sandstones and red mudstones. Local fish teeth and macrovertebrate bone fragments Occurrence: very local; three individual lens-shaped beds (0.1- to 0.4 m-thick) overlying current-ripple cross-laminated sandstones and intercalated with massive and trough cross-bedded fine and medium sandstones, defining fining-upward and coarsening upward units Slightly channeled erosional bases with scour marks and burrows on top	**Flashflood deposits** transporting extraclasts (Aguilar Fm limestones), intraclasts (mudstone rip-up clasts and sandstone clasts) and skeletal remains (Aurell et al., 2016): - fining-upward and coarsening upward units indicate they likely were deposited by several flood events - scour marks and intercalated trough cross-bedded sandstones (i.e. migration of 2-D dunes at lower flow velocities) indicate a SE paleocurrent

S2. Facies description and interpretation of cross-bedded sandstones and poorly bedded conglomerates. Stratigraphic location of sandstone packages (G5, G7 in A), paleocurrent data and paleoenviornmental scheme are shown in Fig. 2 of main text. Grain size results are in Supplementary data S3.

References:

Aurell, M., Bádenas, B., Gasca, J. M., Canudo, J. I., Liesa, C. L., Soria, A. R., ... & Najes, L. (2016). Stratigraphy and evolution of the Galve sub-basin (Spain) in the middle Tithonian–early Barremian: implications for the setting and age of some dinosaur fossil sites. Cretaceous Research, 65, 138-162.

Gibling, R. (2006). Width and Thickness of Fluvial Channel Bodies and Valley Fills in the Geological Record: A Literature Compilation and Classification. Journal of Sedimentary Research 76 (5), 731–770.

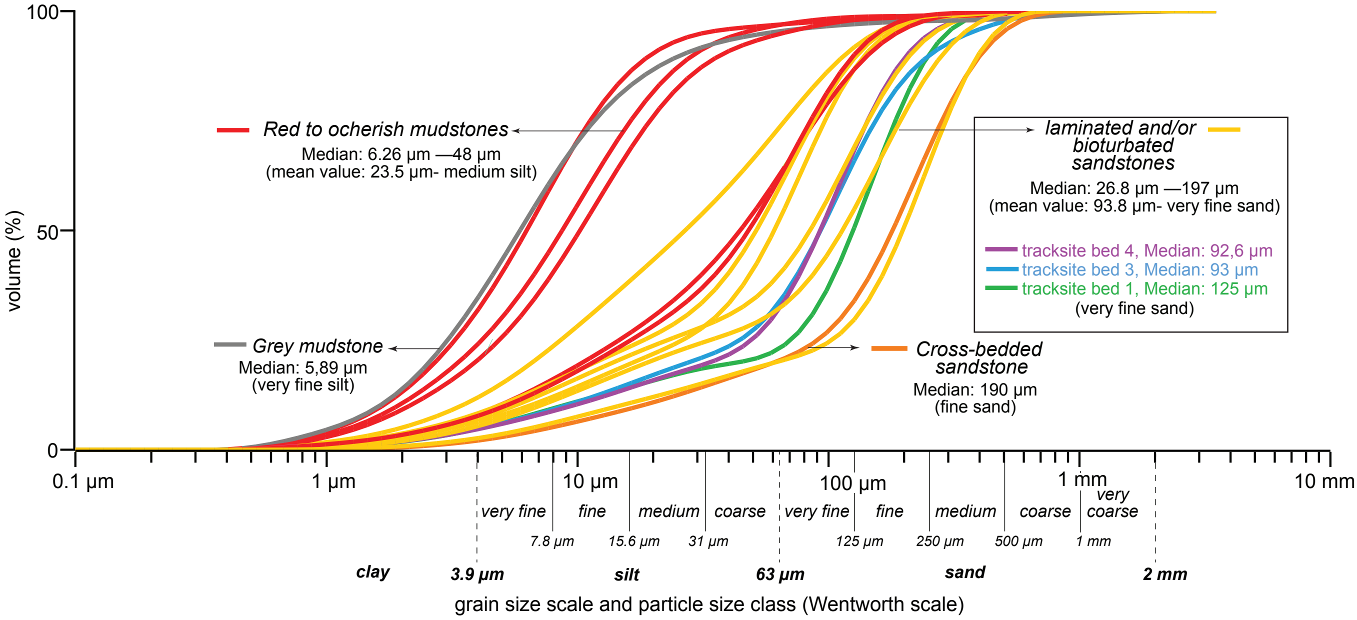

S3. Grain size analysis of muddy and sandy facies of the lower part of the Galve Fm at the *Corrales del Pelejón section*, including the data from beds 1, 3, 4 of the *Los Correles del Pelejón* tracksite. For location of samples see Figs. 2A and 3 of the main text.

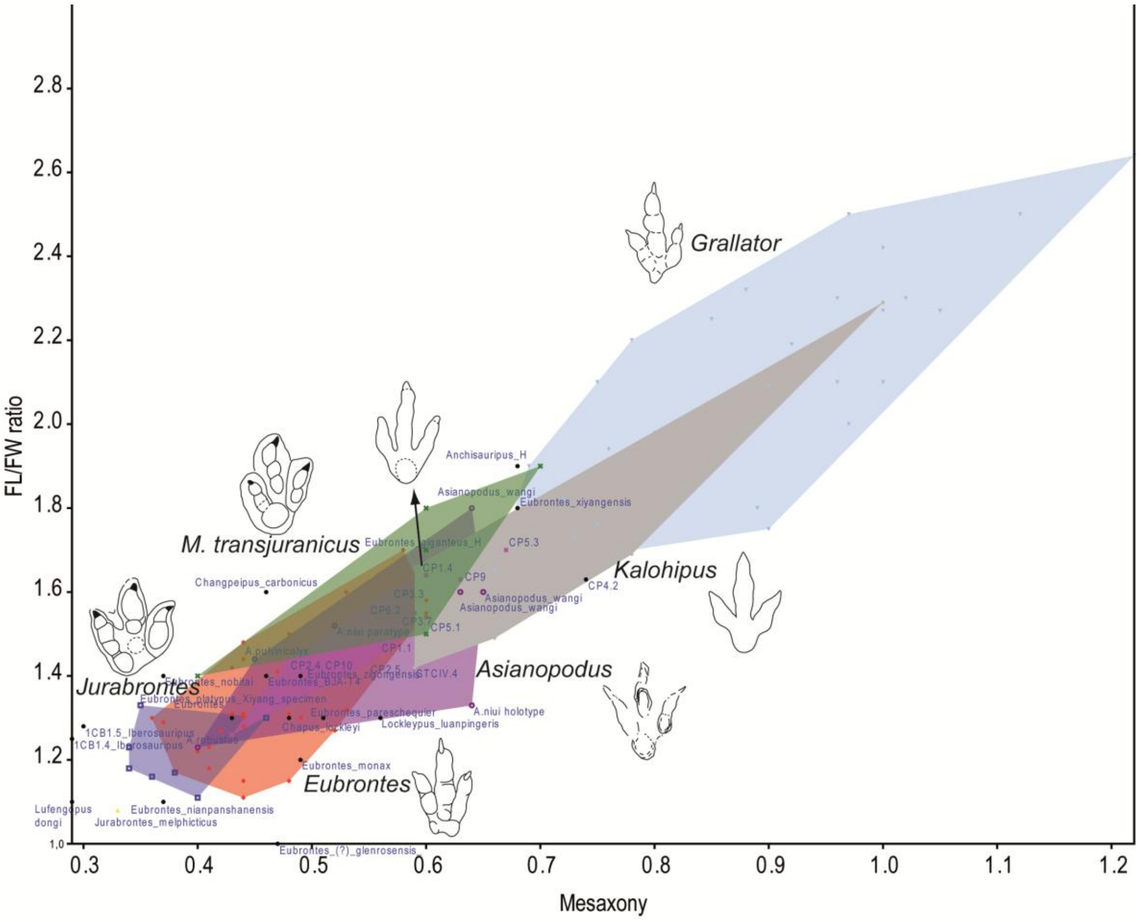

FL/FW ratio
Mesaxony
2.8
2.6
2.4
2.2
2.0
1.8
1.6
1.4
1.2
1,0
0.3
0.4
0.5
0.6
0.7
0.8
0.9
1.0
1.1
1.2
Grallator
M. transjuranicus
Kalohipus
Asianopodus
Jurabrontes
Eubrontes
Anchisauripus_H
Asianopodus_wangi
Eubrontes_xiyangensis
Changpeipus_carbonicus
CP5.3
CP4.2
A.niui holotype
Lockleypus_luanpingeris
Eubrontes_monax
Eubrontes_nianpanshanensis
Jurabrontes_melphicticus
Eubrontes_(?)_glenrosensis
Lufengopus
dongi

TRACK	Left/ right	MP	FL	FW	FL/ FW	LII	LIII	DIII	LIV	WII	WIII	WIV	HPL	HPW	II^III	III^IV	II^IV	ATl	ATw	AT	DIII/FL
CP1.1	left	2	26	17.5	1.48	19	26	19	20	4	5	4	7	6.5	23	23	46	8.5	15	0.56	0.73
CP1.2	right	NP	NP	NP	NP	NP	NP	NP	NP	NP	NP	NP	NP	NP	NP	NP	NP	NP	NP	NP	NP
CP1.3	left	1	25	16.5	1.51	17.5	25	18.5	20	4.5	5	5	6.5	6	23	21	44	7.5	13.5	0.55	0.74
CP1.4	right	2.5	28	17	1.64	19	28	20.5	20.5	4	5	4	7.5	6	22	25	47	9	15	0.6	0.73
CP1.5	left	1	26?	16.5	1.57	17.5	26?	20.5	20.5	4.5	5	5	5.5?	5?	22	24	46	9?	14	0.64	0.78
CP1.6	rigth	0.5	NP	NP	NP	NP	NP	NP	NP	NP	NP	NP	NP	NP	NP	NP	NP	NP	NP	NP	NP
CP2.1	left	1	31	25	1.24	23.5	30	NM	26.5	6	7.5	7	NP	NP	25	27	52	10	20.5	0.48	NM
CP2.2	right	1.5	35?	25.5	1.37	26	35?	NM	27	5.5	6	5.5	NP	NP	26	24	50	10.5?	21.5	0.48?	NM
CP2.3	left	1	36	24.5	1.46	26.5	36	NM	27	5.5	5.5	5	NP	NP	24	23	47	11.5	20	0.57	NM
CP2.4	right	2	37.5	26	1.44	28	37.5	28	29	6.5	7.5	6	9.5	7.5	23	24	47	11	22.5	0.48	0.74
CP2.5	left	2	34.5	24	1.43	25.5	34.5	NM	27	6	6.5	6.5	?	8	26	21	47	11	20	0.55	NM
CP2.6	right	1.5	35.5			26.5?	35.5	29	26.5	6?	6	6	6.5	7.5	23	27	50	10.5	21	0.5	0.81
CP3.1	right	1	27	19	1.42	22	27	NP	23	5	6.5	?	NP	NP	26	18?	44?	6.7	16.5	0.4?	NM
CP3.2	left	1.5	34	22	1.54	22?	34	NM	26.5	5.5	6.5	5.5	NP	NP	23	26	49	12	19	0.63	NM
CP3.3	right	2	35.5	22	1.61	25.5	35.5	25	28	6.5	8.5	6.5	10.5	9.5	23	23	46	11.5	20	0.57	0.70
CP3.4	left	0	32.5	22.5	1.44	NP	NP	NP	NP	NP	NP	NP	NP	NP	NP	NP	NP	NP	NP	NP	NP
CP3.5	right	NP	NP	NP	NP	NP	NP	NP	NP	NP	NP	NP	NP	NP	NP	NP	NP	NP	NP	NP	NP
CP3.6	left	1	34?	23	1.47	23	34?	23	26	5.5	6.5	5.5	11	8.5	24	24	48	12?	20	0.6	0.67
CP3.7	right	2	35	22.5	1.55	27	35	NP	26	5.5	6	5.5	?	?	21	23	44	11	18.5	0.59	NM
CP3.8	left	NM	NM	NM	NM	NM	NM	NM	NM	NM	NM	NM	NM	NM	NM	NM	NM	NM	NM	NM	NM
CP4.1	rigtht	1	13.5?	8.8	1.53	9.5?	13.5?	NP	10	?	?	2	3	3	23	28	51	7.5?	5?	0.66?	NM
CP4.2	left	2?	15.5	9.5	1.63	10.5	15.5	NP	10.5	1.5	2	1.5	?	?	20	25	45	6.3	8.5	0.74	NM

TRACK	Left/ right	MP	FL	FW	FL/ FW	LII	LIII	DIII	LIV	WII	WIII	WIV	HPL	HPW	II^III	III^IV	II^IV	ATl	ATw	AT	DIII/FL
CP5.1	right	2	25.5	16.5	1.54	19.5	25.5	19	19.5	4	4	3.5	6.5	7	24	22	46	8.5	14	0.6	0.74
CP5.2	left	1.5	26	18	1.44	17	26	19.5	19	4.5	5	4.5	6.5	6	27	22	49	10	15	0.66	0.75
CP5.3	right	2	29	17	1.7	20.5	29	22	19	5	5	4	7	5.5	23	22	45	10.5	15.5	0.67	0.75
CP5.4	left	1	24	18	1.3	17	24	NP	19.2	4.5	5	5	NP	NP	25	24	49	8	15	0.53	NM
CP5.5	right	1.5	29	22	1.3	21	29	21	22	5	6	5	8	7	25	27	52	10	18	0.55	0.72
CP5.6	left	1.5	24.5	20	1.2	19?	24.5	NP	20.5	4?	4.5	4	6	6	30	23	53	7.5	17.5	0.42	NM
CP6.1	right	NM	NM	NM	NM	NM	NM	NM	NM	NM	NM	NM	NM	NM	NM	NM	NM	NM	NM	NM	NM
CP6.2	left	2	38.5	24.5	1.57	29.5	38.5	NP	29	5.5	8.5	6.5	?	?	27	19	46	12	21.5	0.55	NP
CP6.3	right	1	39	24.5	1.59	34	39	NP	29	9	9	6	NP	NP	22	20	42	13	21	0.59	NP
CP6.4	left	1	35.5	24.5	1.44	29?	35.5	NP	28.5?	7.5	8	7.5	ND	ND	24	21	45	20.5	13	0.63	NP
CP6.5	right	NM	NM	NM	NM	NM	NM	NM	NM	NM	NM	NM	NM	NM	NM	NM	NM	NM	NM	NM	NM
CP7.1	right	NP	NP	NP	NP	NP	NP	NP	NP	NP	NP	NP	NP	NP	NP	NP	NP	NP	NP	NP	NP
CP7.2	left	NP	NP	NP	NP	NP	NP	NP	NP	NP	NP	NP	NP	NP	NP	NP	NP	NP	NP	NP	NP
CP7.3	right	NM	NM	NM	NM	NM	NM	NM	NM	NM	NM	NM	NM	NM	NM	NM	NM	NM	NM	NM	NM
CP7.4	left	2	35.5	32.5	1.09	28	35.5		27.5	9	9.5	9.5	?	?	28	35	63	12.5	28	0.44	NM
CP8	right	2	28.5	22.5	1.26	22?	28.5	24	22	5	5	4	4.5	5	34	28	62	8.5	19.5	0.43	0.84
CP9	left	2	29.5	18	1.63	20	29.5	21	22	5	5.5	5	8.5	7	23	18	41	9.5	15	0.63	0.71
CP10	left	2	26	18	1.44	19.5?	26	20	20.5	4.5	5	4.5	6	6.5	30	21	51	8	15.5	0.51	0.76
CP11	left	1.5	32	26	1.23	25	32	NP	26	6	5	6	NP	NP	27	25	52	21	9.5	0.45	NP

TRACKWAY	Orientation	PLh	PLt	SLh	SLt	PA	FL	h	Speed* (m/s)	Speed * (Km/h)	Speed ** (m/s)
CP1.1		none	none	2	2	none	0.26				
CP1.2		none	none	none	none	none	NP				
CP1.3		1	1.03	1.98	2	176	0.25				
CP1.4		0.99	0.97	none	none	177?	0.28				
CP1.5		1.08	none	none	none	none	0.26				
CP1.6						none	NP				
Mean	**247**	**1.02**	**1**	**1.99**	**2**	**176.5**	**0.26**	**1.04**	**2.37**	**8.5**	**2.15**
CP2.1		1.09	1.11	2.2	2.27	none	0.31				
CP2.2		1.13	1.17	2.18	2.19	169	0.35				
CP2.3		1.09	1.08	2.2	2.17	167	0.36				
CP2.4		1.13	1.12	2.22	2.2	173	0.37				
CP2.5		1.1	1.12	none	none	174	0.34				
CP2.6						none	0.35				
Mean	**243**	**1.1**	**1.1**	**2.2**	**2.2**	**170.7**	**0.34**	**1.36**	**2.03**	**7.33**	**1.84**
CP3.1		none	1.19	none	2.32	none	0.27*				
CP3.2		1.13	1.16	2.21	none	178	0.34				
CP3.3		none	1.12	none	none	178	0.35				
CP3.4		none	none	2.23	none	none	0.32				
CP3.5		none	none	none	none	none	NP				
CP3.6		1.09	1.12	2.18	none	none	0.34?				
CP3.7		1.1	none	none		170	0.35				
CP3.8					none	none	ND				
Mean	**214**	**1.11**	**1.14**	**2.2**	**2.3**	**175**	**0.34**	**1.36**	**2.19**	**7.9**	**1.98**
CP5.1		none	0.81	none	1.63		0.25				
CP5.2		0.83	0.83	1.6	1.67	none	0.26				
CP5.3		0.77?	0.84	1.67	1.67	175	0.29				
CP5.4		0.86	0.86	1.69	1.66	169	0.24				
CP5.5		0.82	0.82	1.64	1.64	165	0.29				
CP5.6		0.84	0.82	none	none	169	0.24				
Mean	**66**	**0.82**	**0.83**	**1.65**	**1.66**	**169**	**0.27**	**1.08**	**1.66**	**6**	**1.5**
CP6.1		1	1.09	none	2.19	none					
CP6.2		1.07	1.1	2.13	2.14	169	0.38				
CP6.3		1.09	1.07	2.16	2.1	168	0.39				
CP6.4						none	0.35				
Mean	**33**	**1.05**	1.08	**2.14**	**2.14**	**168.5**	**0.37**	**1.48**	**1.76**	**6.33**	**1.59**
CP4.1	**117**	0.79									
CP4.2											
CP7.1	**300**		1.07								
CP7.2											

CP7.3			1.05								
CP7.4											

Speed ** (Km/h)	Relative stride length SL/FL	
		* Alexander 1976 Formula (estimated with SLt)
		** Ruiz and Torices, 2013 Formula (estimated with SLt)
		PLh and SLh = measured from the heel
		PLt and SLt =measured from the tip
7.74	**1.97**	
6.63	**1.57**	
7.14	**1.57**	
5.4	**1.5**	
5.7	**1.42**	
		This trackway has a slight change in direction, and the trackway midline has been estimated